A COLOURFUL CLASSIFICATION OF (QUASI) ROOT SYSTEMS AND HYPERPLANE ARRANGEMENTS

Gabriele Rembado

A COLOURFUL CLASSIFICATION OF (QUASI) ROOT SYSTEMS AND HYPERPLANE ARRANGEMENTS

GABRIELE REMBADO

ABSTRACT. We will introduce a class of graphs with coloured edges to encode subsystems of the classical root systems, which in particular classify them up to equivalence. We will further use the graphs to describe root-kernel intersections, as well as restrictions of root (sub)systems on such intersections, generalising the regular part of a Cartan subalgebra. Finally we will consider a slight variation to encode the hyperplane arrangements only, showing there is a unique noncrystallographic arrangement that arises.

CONTENTS

INTRODUCTION

Let G be a connected complex reductive Lie group, and $T \subseteq G$ a maximal torus (such as the group of invertible diagonal matrices inside $GL_n(\mathbb{C})$). Denote $\mathfrak{g} = \mathrm{Lie}(G)$, and let $\mathfrak{t} = \mathrm{Lie}(T) \subseteq \mathfrak{g}$ be the associated Cartan subalgebra.

A previous paper [16] introduced pure local " wild " mapping class groups of type $\mathfrak{g}$, associated with the root system $\Phi_{\mathfrak{g}} = \Phi(\mathfrak{g}, \mathfrak{t}) \subseteq \mathfrak{t}^\vee$ and some further data: the missing piece comes from moduli spaces arising in complex algebraic geometry, parametrising isomorphism/gauge classes of meromorphic connections on principal G-bundles over a Riemann surface, i.e. the *de Rham* spaces of the wild

2020 *Mathematics Subject Classification.* 17B22,52C35.

Key words and phrases. Root systems, graphs, hyperplane arrangements.

The author is supported by the Deutsche Forschungsgemeinschaft (DFG, German Research Foundation) under Germany Excellence Strategy - GZ 2047/1, Projekt-ID 390685813.

nonabelian Hodge correspondence [3]. See [16] for details and references, in particular the relation with the wild character varieties (the *Betti* spaces) and the admissible deformations of wild Riemann surfaces [8]—as well as the reviews [7, 9]; the "quantum" side of this story, in particular the quantisation of the nonabelian Hodge spaces, has been considered in [21, 22, 23, 17, 1, 2].

The upshot are spaces $\mathbf{B} \subseteq \mathfrak{t}^p$ for an integer $p \geqslant 1$, coming with a product decomposition

$$\mathbf{B} = \prod_{i=1}^{p} \mathbf{B}_i \,, \qquad \mathbf{B}_i \subseteq \mathfrak{t} \,, \tag{1}$$

and the pure local "wild" mapping class group is then the fundamental group

$$\Gamma = \pi_1(\mathbf{B}) \simeq \prod_i \pi_1(\mathbf{B}_i) \,.$$

Now each factor in (1) is a "restricted" root-hyperplane complement, in the following sense. If $\Phi' \subseteq \Phi$ is an inclusion of root systems, we consider the flat

$$\mathfrak{U} \coloneqq \mathrm{Ker}(\Phi') = \bigcap_{\Phi'} \mathrm{Ker}(\alpha) \subseteq \mathfrak{t} \,, \tag{2}$$

of the root-hyperplane arrangement of $\Phi \subseteq \mathfrak{t}^\vee$, and then the complement of the remaining hyperplanes:

$$\mathbf{B}(\Phi', \Phi) \coloneqq \mathfrak{U} \cap \bigcup_{\Phi \setminus \Phi'} \big(\mathfrak{t} \setminus \mathrm{Ker}(\alpha)\big) \subseteq \mathfrak{U} \,. \tag{3}$$

When nonempty, (3) is the complement of the hyperplane arrangement (in $\mathfrak{U}$) obtained upon restriction of the additional roots, i.e.

$$\mathbf{B}(\Phi', \Phi) = \mathfrak{U} \setminus \bigcup_{\Phi \setminus \Phi'} \mathrm{Ker}\big(\alpha|_{\mathfrak{U}}\big) \,. \tag{4}$$

Then there exists an increasing sequence

$$\Phi_1 \subseteq \cdots \subseteq \Phi_{p+1} \coloneqq \Phi_{\mathfrak{g}} \,, \tag{5}$$

of root (sub)systems, such that $\mathbf{B}_i = \mathbf{B}_i(\Phi_i, \Phi_{i+1})$ for $i \in \{1, \ldots, p\}$.

The generic case corresponds to the inclusion $\varnothing \subseteq \Phi_{\mathfrak{g}}$ (for $p = 1$), which brings about the regular part

$$\mathbf{B}(\varnothing, \Phi_{\mathfrak{g}}) = \mathfrak{t}_{\mathrm{reg}} = \mathfrak{t} \setminus \bigcup_{\Phi_{\mathfrak{g}}} \mathrm{Ker}(\alpha) \subseteq \mathfrak{t} \,,$$

of the Cartan subalgebra. Hence this example of local wild mapping class group, whose role in 2d gauge theory was first understood in [4], leads to pure (generalised/Artin–Tits) braid groups of type $\mathfrak{g}$ [12, 14, 13].

The problem we consider here is thus to classify the hyperplane arrangements of the "restricted" systems

$$\Phi|_{\mathfrak{U}} \coloneqq \Big\{ \alpha|_{\mathfrak{U}} \;\Big|\; \alpha \in \Phi \setminus \Phi' \Big\} \subseteq \mathfrak{U}^\vee \tag{6}$$

of linear functionals—in the description (4).

Note (6) is a symmetric subset, but it need *not* be a root system; and further even the resulting hyperplane arrangement is not that of a root system in general—i.e. it is not *crystallographic*. Moreover it is *not* true that the resulting

Coxeter group is obtained by restricting (to U) the elements of the Weyl group preserving (2)—even in type A.

In view of the aforementioned obstructions, an explicit description of (4) in principle relies on a description of:

(1) root subsystems $\Phi \subseteq \Phi_{\mathfrak{g}}$;
(2) for any inclusion $\Phi' \subseteq \Phi$ of two such, the set of equivalence classes of functionals $\alpha, \beta \in \Phi$ with respect to the relation

$$\alpha \sim \beta \qquad \text{if} \qquad U \subseteq \mathrm{Ker}(\alpha - \beta)\,.$$

This latter is also the quotient set $\Phi/U^{\perp} \subseteq \mathfrak{t}^{\vee}/U^{\perp}$, within the quotient vector space (of $\mathfrak{t}^{\vee}$) modulo the annihilator

$$U^{\perp} = \left\{ \lambda \in \mathfrak{t}^{\vee} \;\middle|\; \lambda|_{U} = 0 \right\} \subseteq \mathfrak{t}^{\vee}\,.$$

But in our situation $U^{\perp} = \mathbb{C}\Phi' \subseteq \mathfrak{t}^{\vee}$, so we can equivalently consider the quotient set

$$\Phi/\mathbb{C}\Phi' \subseteq \mathbb{C}\Phi/\mathbb{C}\Phi'\,,$$

which is thus naturally in bijection with (6): we refer to either as the *quotient* of Φ, modulo Φ'. [1]

While a study of such quotients and hyperplane arrangements can be carried in general, the geometric setup of [16] only brings about a particular type of root subsystems: namely the root systems of iterated centraliser of semisimple elements, viz. (reductive) Levi factors of parabolic Lie subalgebras of $\mathfrak{g}$—cf. § 3 of op. cit. These are "fission" root systems [5, 6], and the sequence (5) is then controlled by an increasing sequence of subdiagrams of the Dynkin diagram of the semisimple part $[\mathfrak{g},\mathfrak{g}] \subseteq \mathfrak{g}$, corresponding at each step to the subset of simple roots vanishing on the chosen semisimple element.

In this paper instead we consider *all* root subsystems of a simple Lie algebra $\mathfrak{g}$, which cannot always be read from the Dynkin diagram. This yields the general semisimple case by taking direct products, and finally adding an Abelian factor (in the reductive case) does not modify the homotopy type of (4). [2] More precisely we propose an elementary classification of root subsystems of the classical simple Lie algebras in terms of some combinatoric data: certain graphs with coloured edges which retain more information than the Dynkin diagram, a slight generalisation thereof to describe all possible quotients, and finally a variation to encode the root hyperplanes only.

Note [20] also deals with the classification of irreducible root (sub)systems: in particular the statement of Cor. 4.1 is coherent with the tables in § 10 of op. cit—although for us this comes as a corollary of the main construction, with a more elementary proof, and we further get to *non*crystallographic systems/arrangements by considering quotients.

Finally, using an (invariant) scalar product $(\cdot \mid \cdot)\colon V \otimes V \to \mathbb{C}$, the vanishing locus of a subset $\Phi' \subseteq V^{\vee}$ corresponds to the orthogonal subspace of its image under the vector space isomorphism $(\cdot \mid \cdot)^{\sharp}\colon V^{\vee} \to V$. Then restricting a linear

[1] E.g. if $\Phi' = \{\pm\gamma\}$ for some $\gamma \in \Phi$ then the quotient is the set of γ-strings in Φ.

[2] The (contractible) centre $\mathfrak{z}_{\mathfrak{g}} = \bigcap_{\Phi_{\mathfrak{g}}} \mathrm{Ker}(\alpha) \subseteq \mathfrak{t}$ acts on each factor (1) by translations, and one can appeal to the resulting fibration $\mathfrak{z}^{\mathrm{p}}_{\mathfrak{g}} \hookrightarrow \mathbf{B} \twoheadrightarrow \mathbf{B}/\mathfrak{z}^{\mathrm{p}}_{\mathfrak{g}}$.

functional $\lambda \in V^\vee$ to $U = \mathrm{Ker}(\Phi') \subseteq V$ is the same as taking the orthogonal projection of $(\cdot|\cdot)^\sharp(\lambda) \in V$ onto U: in this viewpoint one is thus led to study projections of (co)roots onto intersections of other (co)roots' kernels (cf. [15]). The viewpoint we take here does not rely on the invariant product, although our results are compatible with the (complex) Euclidean structure (cf. Prop. 5.1).

Main results and layout. In § 1 we review the special linear case, which is the prototype for the other classical types.

In § 2 we introduce *bichromatic* graphs $(\mathcal{G}, c)$, i.e. graphs endowed with a red/green colouring $c\colon \mathcal{G}_1 \to \{R, G\}$ of each edge, and describe the main correspondence which maps them bijectively to symmetric subsets of the nonreduced root system BC_n—if $\mathcal{G}$ has $n \geqslant 1$ nodes, cf. § A. In particular there are "classical" graphs corresponding to root systems of type A, B, C, D and BC, depicted in Ex. 2.1.

In § 3 we introduce a special class of bichromatic graphs, which correspond to (crystallographic) root subsystems of BC_n under the main correspondence above: they are thus called *crystallo*graphs (see Def. 3.1).

Theorem (Cf. Thm. 3.1)**.** *There is a canonical inclusion-preserving bijection between crystallographs on $n \geqslant 1$ nodes and root subsystems of BC_n.*

In § 4 we classify crystallographs directly from their defining properties, proving the following.

Theorem (Cf. Thm. 4.1, Lem. 4.1 and Cor. 4.1)**.** *All crystallographs are disjoint unions of "classical" ones, up to acting on root (sub)systems via the Weyl group; in particular no exceptional types arise from root subsystems of classical simple Lie algebras.*

In § 5 we use crystallographs to explicitly determine the vanishing loci of any root subsystem.

Theorem (Cf. Prop. 5.1)**.** *Let $\Phi \subseteq BC_n$ be a root subsystem, and $\mathcal{G}^\Phi$ the associated crystallograph; then $\mathrm{Ker}(\Phi)$ has a natural basis consisting of the set of type-A connected components of $\mathcal{G}^\Phi$—including trivial ones.*

In § 6 we define "quotients" graphs $\mathcal{G}/\mathcal{G}'$ of nested crystallographs $\mathcal{G}' \subseteq \mathcal{G}$, with the explicit algorithm of Def. 6.1. We study the obstruction for such a quotient to be a crystallograph, and accordingly introduce a weakened notion of *quasi*-crystallographs in Def. 6.2 The main statement about these two new classes of bichromatic graphs is the following.

Theorem (Cf. Thm. 6.1, Thm. 6.2, and Prop. 6.2)**.** *Let $\Phi' \subseteq \Phi \subseteq BC_n$ be nested root systems, and $\mathcal{G}' = \mathcal{G}^{\Phi'}$, $\mathcal{G} = \mathcal{G}^\Phi$ the associated crystallographs. Then the restricted system (6) is associated with the quotient graph $\mathcal{G}/\mathcal{G}'$ under the main correspondence, and it is a quasi-crystallograph; and conversely all quasi-crystallographs arise from quotients of root systems.*

Further we completely classify this extended class of graphs, thereby explicitly describing all possible quotients of root systems.

Theorem (Cf. Cor. 6.1 and Rk. 6.1)**.** *Quasi-crystallographs are disjoint unions of "classical" graphs, and two other "exotic" components—which do* not *generically correspond to root systems.*

In § 7 we modify the main definition to introduce *projective* crystallographs, in Def. 7.2. They retain less information than crystallographs, since are used to (completely) encode the data of subsets of the root-hyperplane arrangement of type B_n/C_n; further a natural "projectification" operation $\mathcal{G} \mapsto \mathbb{P}(\mathcal{G})$ produces such a graph from any crystallograph, and corresponds to taking the canonical projection $\pi\colon V^\vee \setminus \{0\} \to \mathbb{P}(V^\vee)$ of root systems—as their kernels are dilation-independent. Then we adapt the previous arguments to prove the following.

Theorem (Cf. Cor. 7.1 and Thm. 7.1)**.** *Projective crystallographs on $n \geqslant 1$ nodes are in natural inclusion-preserving bijection with root-hyperplane sub-arrangements of $B_n/C_n/BC_n$—and are obtained from the projectification operation on crystallographs. Moreover they are disjoint unions of "classical" projective crystallographs.*

Finally we consider the compatibility of quotients and projectifications, to get to the desired classification of quotient/restricted hyperplane arrangements.

Theorem (Cf. Lem. 7.1 and Thm. 7.2)**.** *Let $\Phi' \subseteq \Phi \subseteq BC_n$ be nested root systems, and $\mathcal{G}' = \mathbb{P}(\mathcal{G}^{\Phi'})$, $\mathcal{G} = \mathbb{P}(\mathcal{G}^{\Phi})$ the associated projective crystallographs. Then the quotient $\mathcal{G}/\mathcal{G}'$ is the projectification of the quasi-crystallograph associated to the restricted system (6), and thus controls the quotient/restricted hyperplane arrangement.*

Moreover all projectifications of quasi-crystallographs are disjoint unions of the "classical" ones, and of a single *exotic component.*

The latter exotic hyperplane arrangement is as follows (cf. [16]). Let $r, s \geqslant 0$ be integers, and consider the standard complex coordinates $z = (z_1, \dots, z_{r+s})$ on $\mathbb{C}^{r+s}$. Then the exotic arrangement contains the hyperplanes

$$H_{ij}^{\pm} = \left\{ z \in \mathbb{C}^{r+s} \;\middle|\; z_i \pm z_j = 0 \right\} \subseteq \mathbb{C}^{r+s}, \qquad i \neq j \in \{1, \dots, r+s\},$$

viz. the root-hyperplanes of type D_{r+s}, plus the hyperplanes

$$H_i = \left\{ z \in \mathbb{C}^{r+s} \;\middle|\; z_i = 0 \right\} \subseteq \mathbb{C}^{r+s}, \qquad i \in \{1, \dots, r\},$$

viz. the root hyperplanes of type B_r/C_r—in the standard embedding $\mathbb{C}^r \hookrightarrow \mathbb{C}^r \times \mathbb{C}^s$.

This arrangement thus plays a distinguished role within the theory of irreducible root systems.

Some standard notions, notations and conventions, used throughout the paper, are summarised in § A.

1. Prototype: type A

The main idea can be seen in type A: let $\mathfrak{g} = \mathfrak{sl}_n(\mathbb{C})$, with root system A_{n-1}.

If $\Phi \subseteq A_{n-1}$ is a root subsystem, for each $i \in \underline{n} := \{1, \dots, n\}$ we can consider the subset

$$I_i = \{i\} \cup \left\{ j \in \underline{n} \;\middle|\; \alpha_{ij}^- \in \Phi \right\} \subseteq \underline{n}, \tag{7}$$

where $\alpha_{ij}^-\colon V \to \mathbb{C}$ are the type-A roots for $V = \mathbb{C}^n$ (cf. § A). The fact that Φ is closed under the root-hyperplane reflections of its elements implies the subsets (7) yield a partition of $\underline{n}$:

$$\underline{n} = \coprod_{i \in J} I_i, \qquad J := \left\{ \min(I_i) \;\middle|\; i \in \underline{n} \right\} \subseteq \underline{n}. \tag{8}$$

In turn there is a root system decomposition

$$\Phi \simeq \bigoplus_J A_{I_i}\,, \qquad A_{I_i} \coloneqq \left\{ \alpha^-_{jk} \;\middle|\; j,k \in I_i \right\} \subseteq \Phi\,. \tag{9}$$

This can be naturally encoded into a graph $\mathcal{G} = \mathcal{G}^\Phi$ on the set of nodes $\mathcal{G}_0 = \underline{n}$, by putting an (unoriented) straight edge $\{j,k\}$ if and only if $\alpha_{jk} \in \Phi$. Then (9) is equivalent to the fact that $\mathcal{G}$ decomposes into a disjoint union

$$\mathcal{G} = \coprod_J \mathcal{G}(i)\,,$$

of (sub)graphs $\mathcal{G}(i) \subseteq \mathcal{G}$ for $i \in J$, each of which is a complete graph on the set of nodes $I_i \subseteq \underline{n}$—without loop edges. Importantly *all* root subsystems are thus parametrised by such graphs.

Moreover one can use these latter to describe quotients, as follows. An inclusion $\Phi' \subseteq \Phi$ corresponds to a subgraph $\mathcal{G}' = \mathcal{G}^{\Phi'}$ of $\mathcal{G}$, on the same set of nodes, and the system of restricted roots (6) is determined by the missing edges. More precisely there may be pairs of connected components $\mathcal{G}'(i), \mathcal{G}'(j) \subseteq \mathcal{G}'$, for $i,j \in J$, such that there are nodes $i_0 \in \mathcal{G}'(i)_0$ and $j_0 \in \mathcal{G}'(j)_0$ which are adjacent in $\mathcal{G}$—i.e. $\{i_0,j_0\} \in \mathcal{G}_1 \setminus \mathcal{G}'_1$; in the next picture the new straight edge (lying in the larger graph only) is depicted by a dashed line:

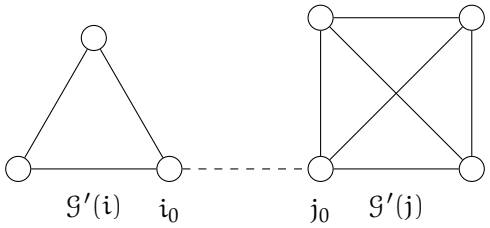

FIGURE 1. Example: two connected components of $\mathcal{G}'$ are linked in $\mathcal{G}$.

Further the fact that Φ is a root (sub)system then implies all pairs of nodes in two such components are adjacent in the larger graph, i.e. there exists a connected component of $\mathcal{G}$ containing both $\mathcal{G}'(i)$ and $\mathcal{G}'(j)$ as subgraphs. This is because the Weyl group element corresponding to $\sigma^-_{ij} \in A_{n-1}$ maps $\alpha^-_{jk} \mapsto \alpha^-_{ki}$, for any triple $\{i,j,k\} \subseteq \underline{n}$ of distinct indices (see below more generally).

Then we can construct a "quotient" graph, denoted $\mathcal{G}/\mathcal{G}'$, with the following algorithm: its set of nodes is that of connected components of $\mathcal{G}'$, viz. the set $J' \subseteq \underline{n}$ associated with Φ' as in (8), and two components are adjacent if and only if they are "fused" in $\mathcal{G}$.

It turns out $\mathcal{G}/\mathcal{G}'$ is still a disjoint union of complete graphs (see below more generally), so it encodes a type-A root system inside $\mathbb{C}^{|J'|}$; and further there is a canonical vector space isomorphism $\mathrm{Ker}(\Phi') \simeq \mathbb{C}^{|J'|}$, identifying A_{n-1} with the root system of $\mathfrak{gl}(V)$—vanishing on the centre $\mathbb{C}\,\mathrm{Id}_V \subseteq \mathfrak{gl}(V)$.

Hence this graph-theoretic description yields in particular a proof of the following:

Proposition 1.1 (Cf. [16])**.**

(1) *If $\Phi \subseteq A_{n-1}$ is a root subsystem, then it is isomorphic to a direct sum of irreducible type-A root systems.*
(2) *If $\Phi' \subseteq \Phi \subseteq A_{n-1}$ is an inclusion of root systems, the quotient Φ/Φ' is isomorphic to a root system of type A, and in particular $A_{n-1}/\Phi' \simeq A_{|J|'-1}$.*

A proof of a stronger statement, involving all classical simple Lie algebras, is given below: in brief a more general class of graphs (extending $\mathcal{G}' \subseteq \mathcal{G}$ and $\mathcal{G}/\mathcal{G}'$ from this section) leads to an explicit description of *all* root subsystems, and of *all* linear functionals that arise upon the restriction (6). The main idea is to add a different type of straight edges to encode the new roots that arise in type D, and further loop edges to encode the short/long roots in type B/C. Finally, at a later time, a variation thereof can be introduced to only encode the resulting hyperplane arrangements (cf. § 7).

Remark 1.1. In particular in type A the "restricted" root-hyperplane complement (4) is identified with a product of spaces of (ordered) configurations of points in the complex affine line, whose fundamental groups are pure braid groups. If $\Phi = A_{n-1}$ there is a single component, and the fundamental group is the pure braid group on $\left|J'\right|$ strands. See [16] about the general case. △

2. Bichromatic graphs and symmetric sets of roots

Let $\{R, G\}$ be the set of colours "red" and "green".

Definition 2.1. A *bichromatic* graph is a graph $\mathcal{G} = (\mathcal{G}_0, \mathcal{G}_1, m)$ equipped with a colour function $c\colon \mathcal{G}_1 \to \{R, G\}$, assigning colours to each edge, such that $c(e, m_e) \neq c(e', m'_e)$ if $e = e' \subseteq \mathcal{G}_0$.

A bichromatic *subgraph* of $(\mathcal{G}, c)$ is a subgraph $\mathcal{G}' \subseteq \mathcal{G}$ equipped with the restricted colour function $c' = c\big|_{\mathcal{G}'_1}$. [3]

The colouring condition is that any two edges incident at the same node(s) have different colours, so there are at most two such edges. We thus say a bichromatic graph is *complete* if it has exactly two edges incident at each pair of (possibly coinciding) nodes.

If the colour function is constant we speak of "red/green graphs" according to whether $c(\mathcal{G}_1) = \{R\}$ or $c(\mathcal{G}_1) = \{G\}$—this is now just an ordinary "monochromatic" graph. We denote $\mathcal{G}_R, \mathcal{G}_G \subseteq \mathcal{G}$ the red/green subgraphs of the bichromatic graph $\mathcal{G}$ obtained by keeping its red/green edges only, i.e. the graphs defined by

$$(\mathcal{G}_\bullet)_0 := \mathcal{G}_0\,, \qquad (\mathcal{G}_\bullet)_1 := c^{-1}(\bullet) \subseteq \mathcal{G}_1\,, \qquad \bullet \in \{R, G\}\,.$$

Clearly all the information about $(\mathcal{G}, c)$ is contained in the pair $(\mathcal{G}_R, \mathcal{G}_G)$.

Recall an ordinary graph is *simply-laced* if it has no repeated edges and no loop edges.

Definition 2.2. A bichromatic graph $(\mathcal{G}, c)$ is *simply-laced* if $(\mathcal{G}_R, \mathcal{G}_G)$ is a pair of simply-laced (monochromatic) graphs.

[3] At times the colour function will be (abusively) omitted.

This means $\mathcal{G}$ has no loop edges, and we denote $\overline{\mathcal{G}} \subseteq \mathcal{G}$ the simply-laced bichromatic graph obtained from $\mathcal{G}$ by removing its loop edges: it is the maximal simply-laced bichromatic subgraph of $\mathcal{G}$. In this terminology a complete bichromatic graph is thus *not* simply-laced, so a *simply-laced complete* bichromatic graph is rather a bichromatic graph with every possible straight edge—but no loop edges.

2.1. **Correspondence with symmetric systems.** Now for an integer $n \geqslant 1$ we use the incidence of a bichromatic graph $(\mathcal{G}, c)$ on the set of nodes $\mathcal{G}_0 = \underline{n}$ to store information about certain subsets of BC_n (cf. § A), in the following (main) correspondence. If $e = \{i, j\} \in \mathcal{G}_1$ is a straight edge, then $\Phi^{\mathcal{G},c}$ contains:

(1) the roots $\pm e_{ij}^-$, if $c(e) = R$;
(2) the roots $\pm e_{ij}^+$, if $c(e) = G$.

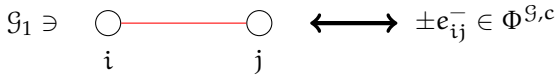

FIGURE 2. Main correspondence, straight edges (I).

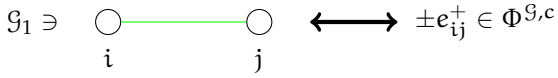

FIGURE 3. Main correspondence, straight edges (II).

Analogously if $l = \{k\} \in \mathcal{G}_1$ is a loop edge of $\mathcal{G}$ then $\Phi^{\mathcal{G},c}$ contains:

(1) the roots $\pm e_k$, if $c(l) = R$;
(2) the roots $\pm 2e_k$, if $c(l) = G$.

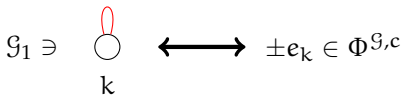

FIGURE 4. Main correspondence, loop edges (I).

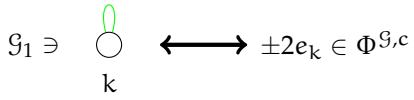

FIGURE 5. Main correspondence, loop edges (II).

By construction $\Phi^{\mathcal{G},c}$ is closed under the involution $\alpha \mapsto -\alpha$ of BC_n—it is a *symmetric* subset. Conversely any symmetric subset $\Phi \subseteq BC_n$ is associated with a unique bichromatic graph $(\mathcal{G}^\Phi, c)$ on n nodes by inverting the above prescription.

By construction these correspondences are mutually inverse order-preserving bijections between bichromatic graphs on $n \geqslant 1$ nodes and symmetric subsets of the root system BC_n.

Example 2.1 (Classical bichromatic graphs). The classical (irreducible) root systems yield the following bichromatic graphs: a simply-laced complete red graph for type A, a simply-laced complete bichromatic graph for type D, a simply-laced complete bichromatic graph with red loop edges (resp. green loop edges) glued at all nodes for type B (resp. type C), and finally a complete bichromatic graph for type BC. See e.g. below for $n = 4$ nodes:

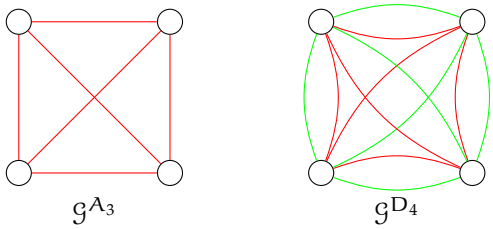

FIGURE 6. Examples of simply-laced classical graphs.

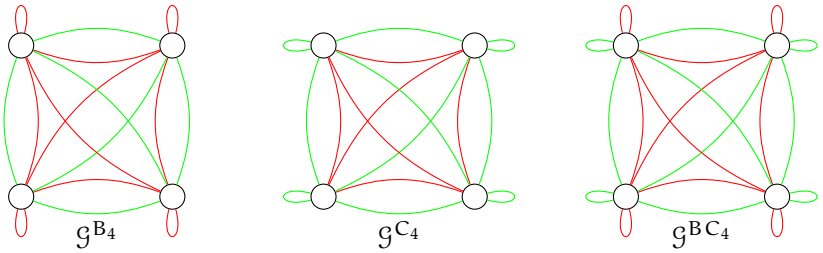

FIGURE 7. Examples of non-simply-laced classical graphs.

△

Remark 2.1 (Dual reading). In this construction $\Phi^{\mathcal{G}}$ is naturally a subset of V, but one may equivalently work with subsets of $V^\vee$ using the dual basis $e_i^\vee$—defined by $\langle e_i^\vee, e_j\rangle = \delta_{ij}$ in the canonical pairing $\langle\cdot,\cdot\rangle : V^\vee \otimes V \to \mathbb{C}$. In this case we consider the linear functionals

$$\alpha_{ij}^{\pm} = e_i^\vee \pm e_j^\vee\,, \quad \alpha_i = e_i^\vee \in V^\vee\,,$$

and again get a bijection $\mathcal{G} \mapsto \Phi^{\mathcal{G}} \subseteq V^\vee$ between bichromatic graphs and symmetric subsets of the dual/inverse root system of BC_n: note $e_i^\vee = (\cdot \mid \cdot)^\flat(e_i) \in V^\vee$ in the isomorphism $(\cdot \mid \cdot)^\flat : V \to V^\vee$ provided by the (canonical) invariant scalar product. The notation is then closer to the prototype in § 1, identifying $V = \mathbb{C}^n$ with the Cartan subalgebra of $\mathfrak{gl}_n(\mathbb{C})$—so the root system lies in the dual. △

3. Crystallographs and main correspondence

The crucial fact is that one can explicitly describe the class of bichromatic graphs that map to root subsystems, rather than arbitrary symmetric subsets of roots. This is achieved by encoding the transformations of roots under mutual root-hyperplane reflections, in the following (main) definition.

Definition 3.1. A bichromatic graph $(\mathcal{G}, c)$ is a *crystallograph* [4] if the following conditions hold:

(1) if a node is incident to two distinct straight edges, then $\mathcal{G}$ contains a straight edge closing the triangle; the third side is red if and only if the first two have the same colour—else it is green;

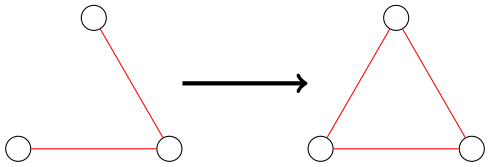

Figure 8. Straight edge closure condition for crystallographs (I).

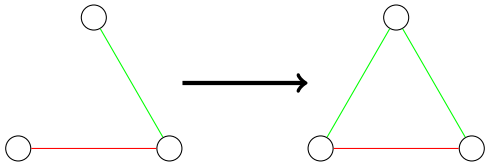

Figure 9. Straight edge closure condition for crystallographs (II).

[4] As in "*crystallo*graphic (bichromatic) *graph*".

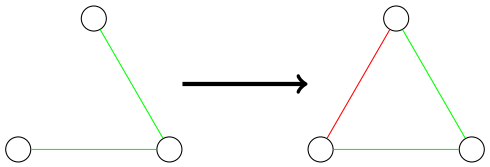

FIGURE 10. Straight edge closure condition for crystallographs (III).

(2) if a node is incident to a loop edge and a straight edge, then $\mathcal{G}$ contains the straight edge of opposite colour, as well as the loop edge of the same colour at the opposite end.

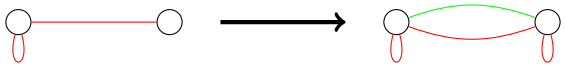

FIGURE 11. Loop edge closure condition for crystallographs (I).

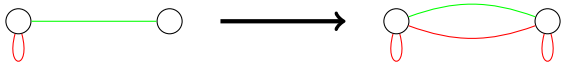

FIGURE 12. Loop edge closure condition for crystallographs (II).

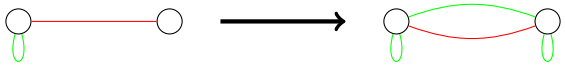

FIGURE 13. Loop edge closure condition for crystallographs (III).

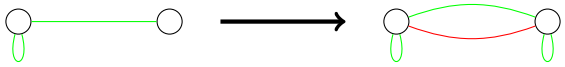

FIGURE 14. Loop edge closure condition for crystallographs (IV).

The fact that the classical root systems of Ex. 2.1 correspond to crystallographs is an intended feature.

Theorem 3.1. *The association* $(\mathcal{G}, c) \mapsto \Phi^{\mathcal{G},c}$ *restricts to a bijection between crystallographs on* $n \geqslant 1$ *nodes and root subsystems of* BC_n.

Proof. The conditions in Def. 3.1 are the translation of the relevant identities for the root-hyperplane reflections.

Namely denote

$$\sigma_{ij}^{\pm} \coloneqq \sigma_{e_{ij}^{\pm}}\,,\ \sigma_i \coloneqq \sigma_{e_i} \in W\big(BC_n\big) \subseteq O\big(V, (\cdot \mid \cdot)\big)\,,$$

for $i \neq j \in \underline{n}$, using the standard notation for Weyl group elements. Then the nontrivial identities are

$$\sigma_{ij}^{-}(e_{jk}^{-}) = e_{ik}^{-}\,, \quad \sigma_{ij}^{-}(e_{jk}^{+}) = e_{ik}^{+}\,, \quad \sigma_{ij}^{+}(e_{jk}^{-}) = -e_{ik}^{+}\,, \quad \sigma_{ij}^{+}(e_{jk}^{+}) = -e_{ik}^{-}\,, \tag{10}$$

and

$$\sigma_i(e_{ij}^{\pm}) = -e_{ij}^{\mp}\,, \qquad \sigma_{ij}^{\pm}(e_j) = \mp e_i\,, \tag{11}$$

for distinct indices $i, j, k \in \underline{n}$.

Thus indeed a bichromatic subgraph $(\mathcal{G}, c)$ is a crystallograph if and only if the associated (symmetric) subset of roots is closed under mutual root-hyperplane reflections: the row of identities (10) corresponds to the former "simply-laced" condition of Def. 3.1 (with $i, j, k \in \mathcal{G}_0$ being the vertices of the triangle), and (11) to the condition involving loop edges (with $i, j \in \mathcal{G}_0$ being the ends of the stright edge). □

Remark 3.1. By construction a crystallograph is connected if and only if the associated root system is irreducible; it is simply-laced if and only if the associated root system is a direct sum of simply-laced irreducible reduced root systems; and it has a double loop edge if and only if the associated root system is nonreduced.

Moreover the bichromatic graph $(\mathcal{G}^{\Phi^\vee}, c^\vee)$ associated with the dual/inverse system is given by $\mathcal{G}^{\Phi^\vee} = \mathcal{G}^{\Phi}$, and then swapping the colour of all loop edges of $(\mathcal{G}^{\Phi}, c)$ (so there is a natural inherited notion of dual/inverse crystallograph).

Finally the *rank* of a crystallograph can be defined by $\mathrm{rk}(\mathcal{G}, c) := \mathrm{rk}(\Phi^{\mathcal{G},c})$, and by construction $\left|\Phi^{\mathcal{G}}\right| = 2|\mathcal{G}_1|$—as every edge corresponds to a pair of opposite roots. △

4. Crystallograph classifications

The point of introducing crystallographs is that one can directly prove the following classification statement.

Theorem 4.1. *Let $(\mathcal{G}, c)$ be a crystallograph on $n \geqslant 1$ nodes. Then $\mathcal{G}$ is a disjoint union of the following types of (crystallo)graphs:*

- *one of the "classical" graphs $\mathcal{G}^{A_{m-1}}$, $\mathcal{G}^{D_m}$, $\mathcal{G}^{B_m}$, $\mathcal{G}^{C_m}$, $\mathcal{G}^{BC_m}$, with $m \leqslant n$;*
- *a bichromatic graph $\mathcal{G}^{d_1,d_2}$ on nodes $\mathcal{G}_0^{d_1,d_2} = I_1 \amalg I_2$, with $|I_i| = d_i$ and $d_1 + d_2 \leqslant n$, such that $\mathcal{G}_R^{d_1,d_2} = \mathcal{G}^{A_{d_1-1}} \amalg \mathcal{G}^{A_{d_2-1}}$ and $\mathcal{G}_G^{d_1,d_2}$ has one straight edge between every pair of nodes lying in different parts—and none other.*

The green part of $\mathcal{G}^{d_1,d_2}$ is thus a (monochromatic, simply-laced) complete bipartite graph on the set of nodes $I_1 \amalg I_2$; see an example below:

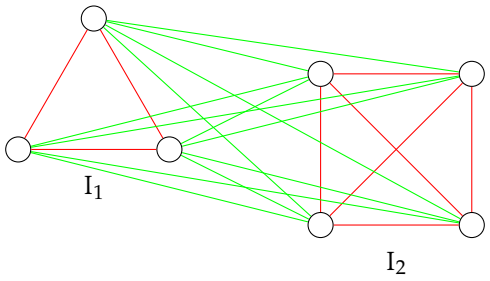

FIGURE 15. Example: a graph of type $\mathcal{G}^{d_1,d_2}$ (for $(d_1, d_2) = (3, 4)$).

Proof. Let us first suppose $\mathcal{G}$ is simply-laced, which involves the first condition of Def. 3.1.

That condition implies that if two nodes are the endpoints of a path of red edges, then they are the endopoints of a red edge, upon completing a sequence of red triangles:

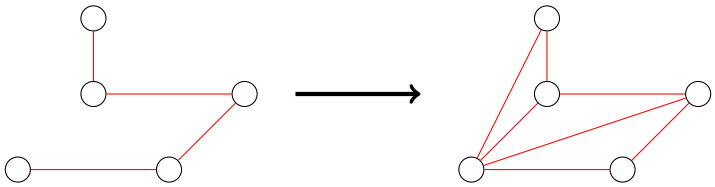

FIGURE 16. Example: completing red triangles along a red path.

Thus $\mathcal{G}_R$ splits into a disjoint union of simply-laced complete graphs. Further adding a green edge within such a component turns this latter into a simply-laced complete bichromatic graph, upon completion of some triangles—both red and green:

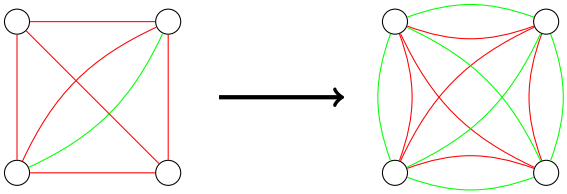

FIGURE 17. Example: completing triangles within a red component.

Thus at this stage $\mathcal{G}$ splits as a disjoint union of type-A (= red) and type-D (= bichromatic) components, and we can in principle further add green edges between two such. Reasoning as above shows that if there is a green edge between two nodes lying in different red components, then all pairs of nodes lying in the two different parts will be the endpoints of a green edge:

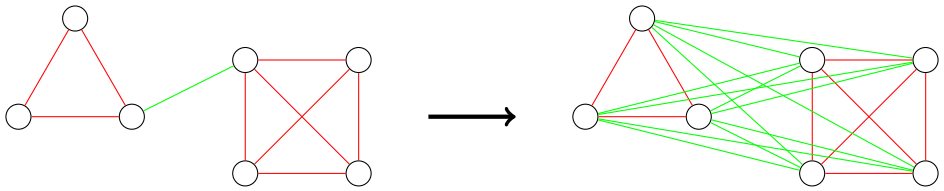

FIGURE 18. Example: completing triangles between two red components.

Analogously if a green edge is drawn from a bichromatic component to either a red or a bichromatic one, then both will be "fused" into a single bichromatic component—as all green edges will propagate.

Finally suppose there is a node of a red component, which is linked to two different red components via green edges. A final application of the "simply-laced" condition of Def. 3.1 shows the two latter red components are then fused into a single red one, creating a graph of type $\mathcal{G}^{d_1,d_2}$:

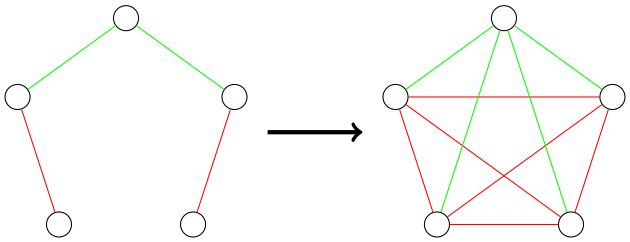

FIGURE 19. Example: completing triangles among triples of red components.

We conclude that $\mathcal{G}$ splits into a disjoint union of the simply-laced components of the statements.

To conclude the proof for a generic graph, note glueing a loop edge to a node in any component of $\overline{\mathcal{G}}$ turns this latter into a simply-laced complete bichromatic graph, having a loop edge of the same colour at each node—by the second condition of Def. 3.1. □

Remark 4.1. In view of Thm. 4.1 we can talk of the "red components" of a crystallograph: these are the type-A subgraphs that appear in his decomposition, i.e. the simply-laced complete red graphs it contains. By convention a trivial component, consisting of a disconnected node, is also considered to be red. [5]

These red components play a central role in the computation of root-kernel intersection, see § 5; and the presence/absence of trivial components in turn controls quotients of root systems, see § 6.

By the same token, a "bichromatic" component is a connected component of any other type B, C, D or BC. △

Now we consider the simply-laced bichromatic graphs $\mathcal{G}^{d_1,d_2}$, for $d_i \geqslant 1$; let simply $\Phi^{d_1,d_2} := \Phi^{\mathcal{G}^{d_1,d_2}} \subseteq \mathrm{BC}_n$.

[5] It corresponds to the "rank-zero" root system $A_0 = \varnothing$.

Lemma 4.1. *The root system* Φ^{d_1,d_2} *is equivalent to* $A_{d_1+d_2-1}$*—inside* BC_n.

Proof. For $i \in I_1$ consider the element $\sigma_i = \sigma_{e_i} \in W(BC_{d_1+d_2})$. This is an orthogonal transformation of $\mathbb{C}^{d_1+d_2}$, and it will turn Φ^{d_1,d_2} into a different root subsystem of $BC_{d_1+d_2}$ as follows (using (11)): the crystallograph associated with $\sigma_i(\Phi^{d_1,d_2})$ is obtained by changing the colour of all edges incident at the node $i \in I_1$.

The result is a graph of type $\mathcal{G}^{d_1-1,d_2+1}$, since i will now be part of a bigger red component on nodes $I_2 \amalg \{i\}$. [6]

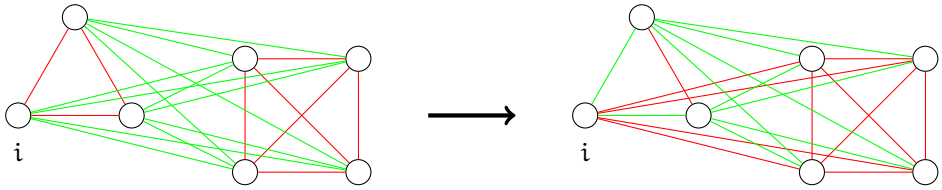

FIGURE 20. Example: Weyl reflection at a node i of $\mathcal{G}^{3,4}$ (turning it into $\mathcal{G}^{2,5}$).

Then repeating at all nodes of $I_1 \subseteq \mathcal{G}_0^{d_1,d_2}$ yields a transformation

$$w = \prod_{I_1} \sigma_i \in W(BC_{d_1+d_2}), \tag{12}$$

after choosing a total order for I_1. By construction the Weyl element (12) turns $\mathcal{G}^{d_1,d_2}$ into the simply-laced complete red graph on nodes $I_1 \amalg I_2$, which is associated with the root subsystem $A_{d_1+d_2-1}$ by the main correspondence. □

Remark 4.2. One can also show (in nonconstructive fashion) that Φ^{d_1,d_2} is isomorphic to $A_{d_1+d_2-1}$.

First, by Thm. 3.1, Φ^{d_1,d_2} is an irreducible reduced simply-laced root system, so it must be of type A, D or E. Now the number of edges of $\mathcal{G}^{d_1,d_2}$ equals

$$\left|\mathcal{G}_1^{d_1,d_2}\right| = \binom{d_1}{2} + \binom{d_2}{2} + d_1 d_2 = \binom{d_1+d_2}{2}.$$

Then one can show that $(\Phi^{d_1,d_2})^\perp = \mathbb{C}v$, as a subspace of

$$\mathbb{C}^{d_1+d_2} \simeq \bigoplus_{i \in \mathcal{G}_0^{d_1,d_2}} \mathbb{C}e_i \subseteq \mathbb{C}^n,$$

with the restriction of the standard scalar product of V, where

$$v := \sum_{I_1} e_i - \sum_{I_2} e_i \in \mathbb{C}^{d_1+d_2}.$$

Hence Φ^{d_1,d_2} has rank equal to $\dim(\mathbb{C}\Phi^{d_1,d_2}) = d_1 + d_2 - 1$, and it contains $2\left|\mathcal{G}_1^{d_1,d_2}\right| = (d_1+d_2)(d_1+d_2-1)$ roots: it must be isomorphic to $A_{d_1+d_2-1}$. △

[6] There are $d_1 - 1$ red edges incident at $i \in I_1$, and d_2 incident green edges, so this operation is *not* symmetric with respect to the two parts.

Note the Weyl element (12) preserves the orthogonal complement of $\mathbb{C}^{d_1+d_2} \subseteq \mathbb{C}^n$, so the other components of the graph are unaffected. If one only considers root subsystems up to equivalence, it is then enough to work with disjoint unions of "classical" crystallographs: indeed the "inner" automorphisms suffice to turn any crystallograph into a union of those—by Thm. 4.1 and Lem. 4.1.

Putting all together we have thus in particular proved the following statement.

Corollary 4.1. *Suppose $\Phi' \subseteq \Phi \subseteq \mathrm{BC}_n$ are nested root systems. Then:*

- *if $\Phi = \mathrm{A}_n$, Φ' is equivalent to a direct sum of type-*A *irreducible root systems;*
- *if $\Phi = \mathrm{D}_n$, Φ' is equivalent to a direct sum of type-*A *and type-*D *irreducible root systems;*
- *if $\Phi = \mathrm{B}_n$, Φ' is a equivalent to a direct sum of type-*A*, type-*D *and type-*B *irreducible root systems;*
- *if $\Phi = \mathrm{C}_n$, Φ' is equivalent to a direct sum of type-*A*, type-*D *and type-*C *irreducible root systems.*

This is coherent with the tables of [20, § 10]—with a different, more elementary proof.

5. Root-kernel intersections

Crystallographs can also be used to describe kernel intersections of arbitrary root subsystems $\Phi \subseteq \mathrm{BC}_n$, generalising the prototype of § 1.

To this end let us work in the dual viewpoint where $\Phi^{\mathcal{G},c} \subseteq V^\vee$ for any bichromatic graph $(\mathcal{G}, c)$. Let then J be the set of red components of $\mathcal{G}$, as in Rk. 4.1, and denote $I_j \coloneqq \mathcal{G}(j)_0 \subseteq \mathcal{G}_0$ the set of nodes of the component $\mathcal{G}(j) \subseteq \mathcal{G}$—for $j \in J$. Finally write $I_R = \coprod_{j\in J} I_j \subseteq \mathcal{G}_0$ the set of nodes of all red components.

Proposition 5.1 (Cf. [16])**.** *If $\mathcal{G}_0 = \underline{n}$ then there is a canonical vector space isomorphism $\mathbb{C}^{|J|} \simeq \mathrm{Ker}\big(\Phi^{\mathcal{G},c}\big)$, given by*

$$\overline{e}_j \longmapsto \nu_{I_j} = \frac{e_{I_j}}{|I_j|}\,, \qquad e_{I_j} \coloneqq \sum_{i\in I_j} e_i \in V\,, \tag{13}$$

denoting $(\overline{e}_j)_j$ the canonical basis of $\mathbb{C}^{|J|}$.

Moreover the map $\pi_U \colon V \to V$ defined by

$$e_i \longmapsto \begin{cases} \nu_{I_i}\,, & i \in I_R \\ 0\,, & i \notin I_R \end{cases}$$

is the orthogonal projection onto $\mathrm{Ker}\big(\Phi^{\mathcal{G},c}\big) \subseteq V$, where $I_i \subseteq I_R$ is the (unique) part containing the node $i \in \underline{n}$—if it exists.

Note the vectors ν_{I_j} yield an orthonormal basis of the kernel, endowed with the restriction of the canonical scalar product.

Proof. The kernel is obtained by intersecting:

- $\mathrm{Ker}(\alpha_{ij}^-)$, if $\{i,j\} \in \mathcal{G}_1$ is red;
- $\mathrm{Ker}(\alpha_{ij}^+)$, if $\{i,j\} \in \mathcal{G}_1$ is green;
- $\mathrm{Ker}(\alpha_i)$, if $\{i\} \in \mathcal{G}_1$ is a loop edge.

Hence any loop annihilates the generator $e_i \in V$, and the same is true of $e_i, e_j \in V$ if $(\mathcal{G}, c)$ contains both a red and a green straight edge $\{i, j\}$. Thus only generators attached to nodes in red components survive in the kernel intersection.

Conversely, if there is a red component on nodes $I_k \subseteq \mathcal{G}_0$, then (in the kernel) the coordinates along the vectors e_i and e_j are equal for all $i, j \in I_k$, which yields the line generated by the vector e_{I_j} of (13).

As for the second statement, one directly checks that $\pi_U\big|_U = \mathrm{Id}_U$ and

$$(\pi_U(v) \mid u) = (v \mid u)\,, \qquad v \in V\,,\, u \in U\,. \qquad \square$$

6. Classification of quotients

Finally we can make further use of crystallographs to describe quotients of root systems, which is one of the main motivations.

Consider thus the situation where $\mathcal{G}' \subseteq \mathcal{G}$ is an inclusion of crystallographs on $n \geqslant 1$ nodes. By Thm. 4.1 and Lem. 4.1 we can assume both are disjoint union of graphs of type A, B, C, D and BC, up to acting via the Weyl group.

By an "edge between two components" we mean a straight edge drawn between a pair of nodes lying in two distinct connected components; analogously a "straight edge within a component" is a straight edge between a pair of nodes lying within one component, and a "loop in a component" is a loop at any node within a component.

Definition 6.1. The *quotient* graph $\mathcal{G}/\mathcal{G}'$ is the bichromatic graph whose nodes are given by the set $\{\mathcal{G}'(j)\}_{j\in J}$ of red components of $\mathcal{G}'$, and whose adjacency/colouring is defined as follows:

- if there is a straight edge $e \in \mathcal{G}_1$ between two red components $\mathcal{G}'(i)$ and $\mathcal{G}'(j)$ of $\mathcal{G}'$, put a straight edge $\{\mathcal{G}'(i), \mathcal{G}'(j)\}$ of the same colour;
- if there is a straight green edge $e \in \mathcal{G}_1$ within one red component $\mathcal{G}'(i)$ of $\mathcal{G}'$, put a green loop $\{\mathcal{G}'(i)\}$;
- if there is a straight edge $e \in \mathcal{G}_1$ from one red component $\mathcal{G}'(i)$ of $\mathcal{G}'$ to a bichromatic component of $\mathcal{G}'$, put a red loop $\{\mathcal{G}'(i)\}$;
- if there is a loop $l \in \mathcal{G}_1$ in a red component $\mathcal{G}'(i)$ of $\mathcal{G}'$, put a loop $\{\mathcal{G}'(i)\}$ of the same colour.

Example 6.1 (Adjacency of a quotient of crystallographs). In the following pictures, which exemplify all cases of Def. 6.1, we represent by dashed lines the edges lying in $\mathcal{G}_1 \setminus \mathcal{G}'_1 \subseteq \mathcal{G}_1$.

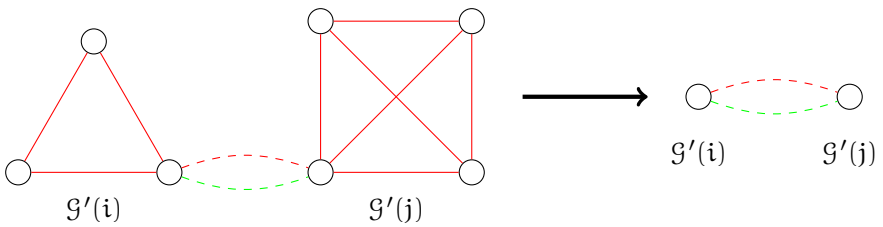

Figure 21. Example: straight edge in $\mathcal{G}/\mathcal{G}'$, arising from a straight edge between two red components of $\mathcal{G}'$.

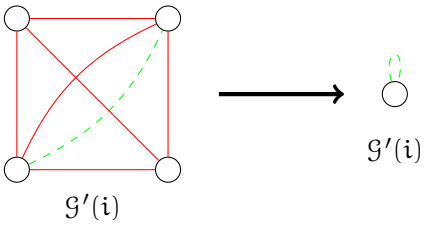

FIGURE 22. Example: green loop edge in $\mathcal{G}/\mathcal{G}'$, arising from a green straight edge within a red component of $\mathcal{G}'$.

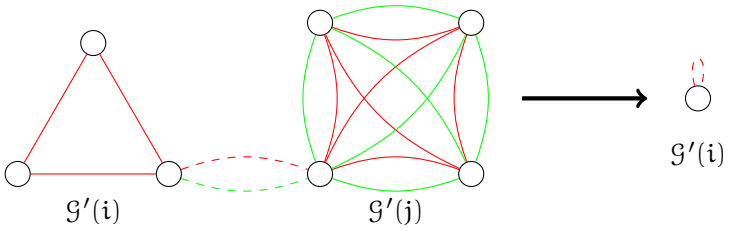

FIGURE 23. Example: red loop edge in $\mathcal{G}/\mathcal{G}'$, arising from a straight edge from a red component to a bichromatic component of $\mathcal{G}'$.

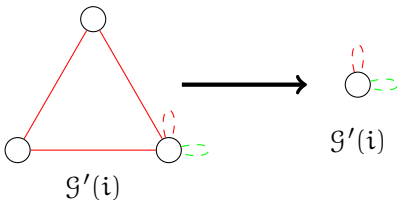

FIGURE 24. Loop edge in $\mathcal{G}/\mathcal{G}'$, arising from a loop edge within a red component of $\mathcal{G}'$.

△

Now let $U \coloneqq \mathrm{Ker}\big(\Phi^{\mathcal{G}'}\big) \subseteq V$, and consider the restriction of all other (co)roots $\alpha \in \Phi^{\mathcal{G}} \setminus \Phi^{\mathcal{G}'}$ to U: this yields the set (6). Clearly this set of restricted functionals is symmetric, so by the main correspondence it is associated with a bichromatic graph on as many nodes as $\dim(U) \leqslant n$; but by Prop. 5.1 this dimension is the number of red components of $\mathcal{G}'$, which in turn is the set of nodes of the quotient graph in Def. 6.1: the next statement thus motivates that definition.

Theorem 6.1. *One has* $\Phi^{\mathcal{G}/\mathcal{G}'} = \Phi^{\mathcal{G}}\big|_U \subseteq U^\vee$.

Proof. This follows directly by evaluating all covectors $\alpha_{ij}^{\pm}, \alpha_i \in V^\vee$ on the vectors $e_{I_k} \in V$ in (13), which provide a basis of U, and then expressing the restrictions $\alpha_{ij}^{\pm}|_U, \alpha_i|_U \in U^\vee$ in terms of the dual basis $e_{I_k}^\vee$. Note this latter is an orthonormal basis of $U^\vee$ for the dual scalar product, since $e_{I_k}^\vee$ is mapped to the normalised vector $v_{I_k} = \frac{e_{I_k}}{|I_k|} \in V$ under the isomorphism $(\cdot \mid \cdot)^\sharp \colon V^\vee \to V$. □

As a corollary we not only derive the type-A case of § 1, where the quotient root systems are still root systems, but also verify that this is false in general: the quotient graph is *not* always a crystallograph, e.g. in the following situation—corresponding to the root-system inclusion $A_1 \subseteq D_4$:

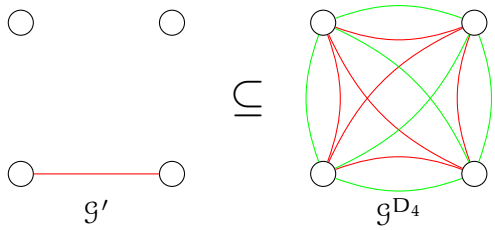

In this case the resulting arrangement consists of seven hyperplanes in $\mathbb{C}^3$, so it is *not* crystallographic (cf. § 7).

Nonetheless the algorithm of Def. 6.1 yields the general way to encode all (sub)quotients of classical irreducible root systems, and moreover it is possible to explicitly describe the class of bichromatic graphs one obtains.

6.1. **Crystallographic obstruction.** Here we study the obstruction for a quotient graph $\mathcal{G}/\mathcal{G}'$ to be a crystallograph. The result is that *all but one* condition of Def. 3.1 apply.

Definition 6.2. A *quasi-crystallograph* is a bichromatic graph $(\mathcal{G}, c)$ satisfying all conditions of Def. 3.1, with the following exception: if a straight edge and a green loop edge are incident at a common node, then the green loop edge need *not* propagate at the other end of the straight edge—but the straight edge will double.

Compare the next two figures with Figg. 13 and 14.

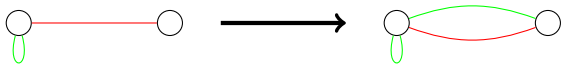

FIGURE 25. Green loop edge closure condition for quasi-crystallographs (I).

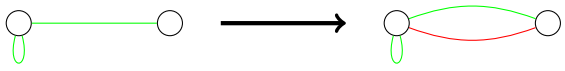

FIGURE 26. Green loop edge closure condition for quasi-crystallographs (II).

Theorem 6.2. *All quotient graphs are quasi-cristallographs.*

We will prove this statement with a case-by-case analysis of the crystallograph conditions. In all the following local pictures we depict edges lying in $\mathcal{G}_1 \setminus \mathcal{G}'_1$ with dashed lines—as above.

Proposition 6.1. *The simply-laced part of any quotient graph is a crystallograph.*

Hence by Thm. 4.1 it will be a disjoint union of graphs of type A and D.

Proof. We must prove the first condition of Def. 3.1 is satisfied for any pair of crystallographs $\mathcal{G}' \subseteq \mathcal{G}$, i.e. that suitable triangles close in the quotient.

Suppose then we have two consecutive straight red edges $\{\, \mathcal{G}'(i), \mathcal{G}'(j) \,\}$ and $\{\, \mathcal{G}'(j), \mathcal{G}'(k) \,\}$ in $\mathcal{G}/\mathcal{G}'$, for $i, j, k \in J$. This means there are red straight edges $\{\, i_0, j_0 \,\}, \{\, \widetilde{j}_0, k_0 \,\} \in \mathcal{G}_1 \setminus \mathcal{G}'_1$ (in $\mathcal{G}$) such that $i_0 \in \mathcal{G}'(i)_0$, $j_0, \widetilde{j}_0 \in \mathcal{G}'(j)_0$ and $k_0 \in \mathcal{G}'(k)_0$:

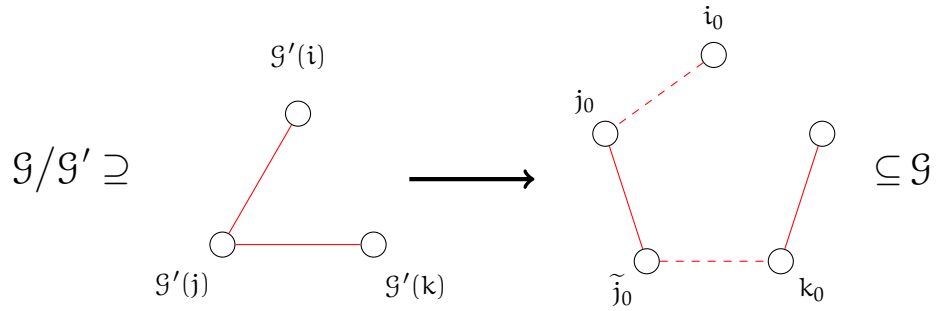

FIGURE 27. Example: completing a red triangle in the quotient (I).

But since $\mathcal{G}$ is a crystallograph these three red components of $\mathcal{G}'$ are then contained in a single component of $\mathcal{G}$:

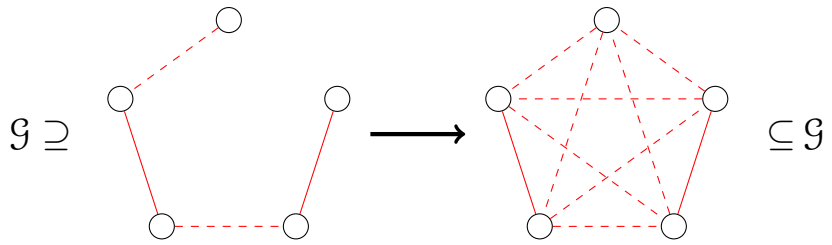

FIGURE 28. Example: completing a red triangle in the quotient (II).

In particular $\{\, i_0, k_0 \,\} \in \mathcal{G}_1 \setminus \mathcal{G}'_1$ and the red triangle closes in the quotient:

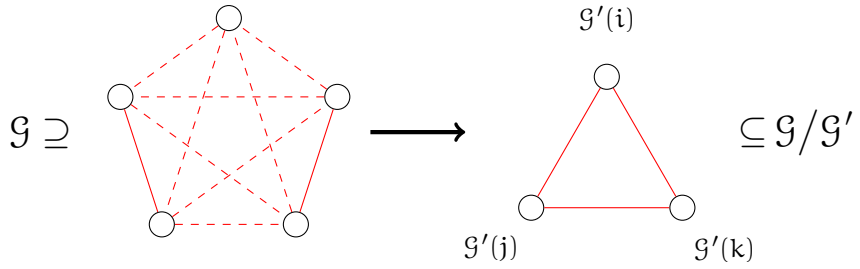

FIGURE 29. Example: completing a red triangle in the quotient (III).

Analogous arguments work in the cases where there are two consecutive straight edges of green/different colour. □

This is coherent with the fact that all quotients of type-A crystallographs are crystallographs (of type-A)—and strengthens it.

Lemma 6.1. *The second condition of Def. 3.1 is verified for red loop edges in* $\mathcal{G}/\mathcal{G}'$.

In particular if the quotient has no green loop edges then it is a crystallograph: by Thm. 4.1 it will be a disjoint union of graphs of type A, D and B.

Hereafter a yellow straight edge (in a picture) stands for a straight edge of either colour. [7]

Proof. Suppose there is a red loop edge $\{\mathcal{G}'(i)\}$ at a node of the quotient, and a straight edge $\{\mathcal{G}'(i), \mathcal{G}'(j)\}$ incident at the same node, for $i, j \in J$. Then we have a straight edge $\{i_0, j_0\} \in \mathcal{G}_1 \setminus \mathcal{G}'_1$ (in $\mathcal{G}$) with $i_0 \in \mathcal{G}'(i)_0$ and $j_0 \in \mathcal{G}'(j)_0$, and one of the following two cases:

(1) the component $\mathcal{G}'(i)$ has red loop edges in $\mathcal{G}$;

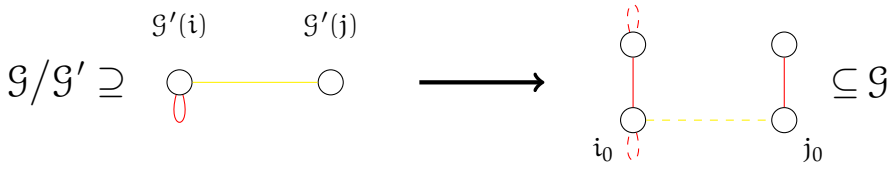

FIGURE 30. Example: red loop edge closure condition for quotients, first case (I).

(2) there is a straight edge $\{\widetilde{i}_0, k_0\} \in \mathcal{G}_1 \setminus \mathcal{G}'_1$ (in $\mathcal{G}$) such that $k_0 \in \mathcal{G}_0$ lies within a bichromatic component of $\mathcal{G}'$.

[7] Recall $Y = R + G$ in the additive RGB colour model.

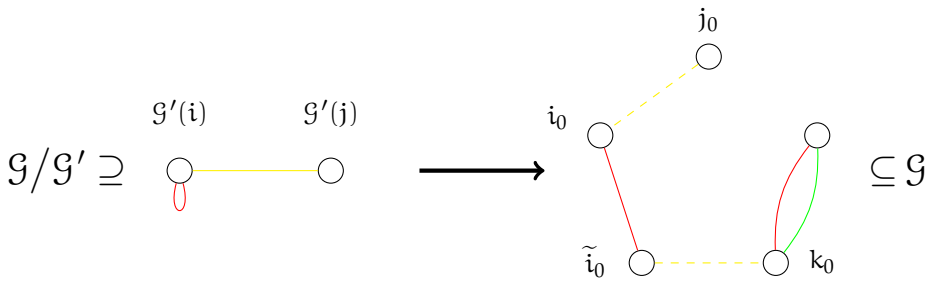

FIGURE 31. Example: red loop edge closure condition for quotients, second case (I).

In the first case the red loop edges propagate to the nodes of $\mathcal{G}'(j) \subseteq \mathcal{G}'$, since $\mathcal{G}$ is a crystallograph, and moreover the straight edge $\{ i_0, j_0 \}$ will "double" (in $\mathcal{G}$):

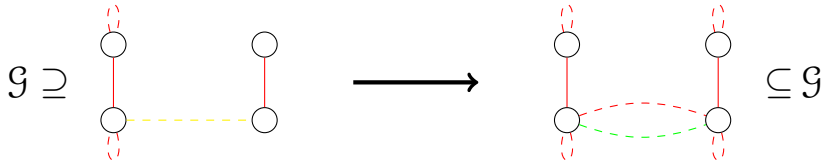

FIGURE 32. Example: red loop edge closure condition for quotients, first case (II).

Hence the same will happen in the quotient:

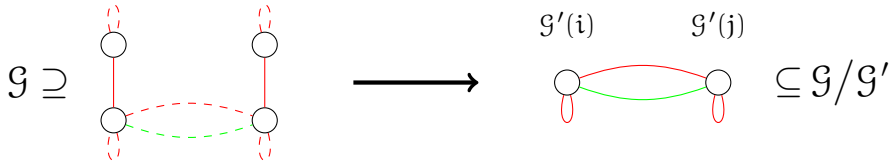

FIGURE 33. Example: red loop edge closure condition for quotients, first case (III).

In the second case the red component $\mathcal{G}'(i) \subseteq \mathcal{G}'$ is contained within a bichromatic component of $\mathcal{G}$ (since it is linked to a bichromatic component of $\mathcal{G}'$ by a straight edge); then analogously the subgraph $\mathcal{G}'(j) \subseteq \mathcal{G}'$ is also contained in that bichromatic component of $\mathcal{G}$:

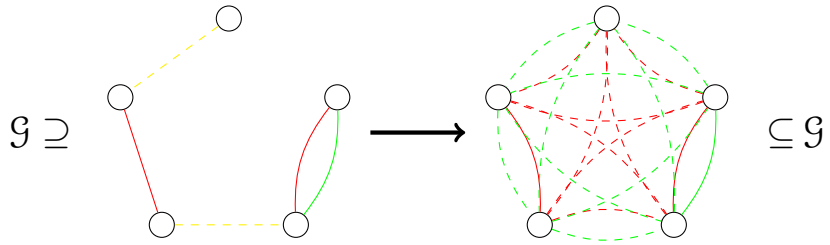

FIGURE 34. Example: red loop edges closure condition for quotients, second case (II).

In particular there is a straight edge $\{j_0, k_0\} \in \mathcal{G}_1 \setminus \mathcal{G}'_1$ that yields a red loop $\{\mathcal{G}'(j)\}$ in the quotient, as well as a straight edge of opposite colour $\{i_0, j_0\}$, which lead to the required crystallographic configuration in the quotient:

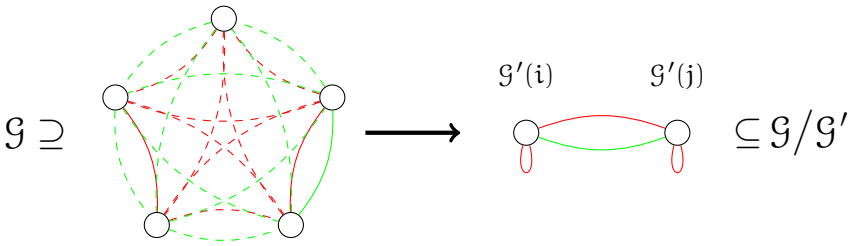

FIGURE 35. Example: red loop edges closure condition for quotients, second case (III).

□

Let us finally consider *green* loop edges: suppose there is a green loop edge at a node of the quotient $\mathcal{G}/\mathcal{G}'$, and a straight edge incident to it.

Lemma 6.2. *If a green loop edge $\{\mathcal{G}'(i)\}$ in the quotient originates from green loop edges at the nodes of the red component $\mathcal{G}'(i) \subseteq \mathcal{G}'$, then the second condition of Def. 3.1 is verified for $\mathcal{G}/\mathcal{G}'$.*

Proof. This follows as in the proof of the first case in the previous Lem. 6.1; compare the following sequence of pictures with Figg. 30, 32 and 33:

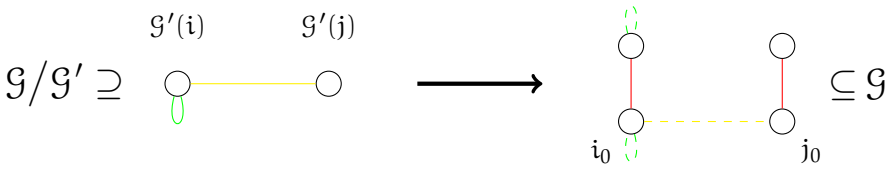

FIGURE 36. Example: green loop edge closure condition for quotients, first case (I).

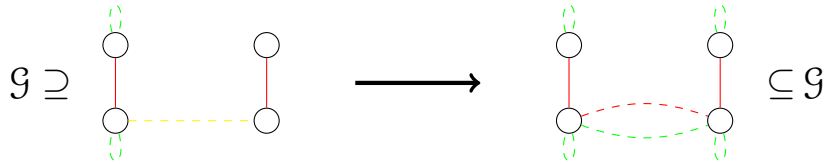

FIGURE 37. Example: green loop edge closure condition for quotients, first case (II).

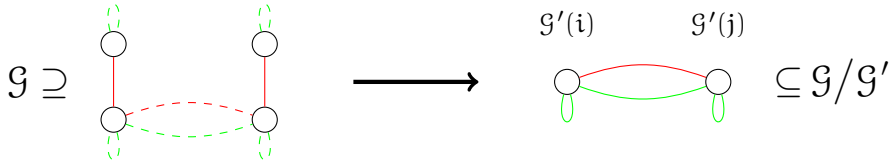

FIGURE 38. Example: green loop edge closure condition for quotients, first case (III).

□

The final case is the following: there is a red component $\mathcal{G}'(i) \subseteq \mathcal{G}'$ such that there exists a green straight edge $\{i_0, \widetilde{i}_0\} \in \mathcal{G}_1 \setminus \mathcal{G}'_1$ for (distinct) nodes $i_0, \widetilde{i}_0 \in \mathcal{G}'(i)_0$, and $\mathcal{G}'(i)$ is connected by a straight edge $\{\bar{i}_0, j_0\} \in \mathcal{G}_1 \setminus \mathcal{G}'_1$ to another red component $\mathcal{G}'(j) \subseteq \mathcal{G}'$. In this case we must distinguish the case where $\mathcal{G}'(j)$ is trivial or not:

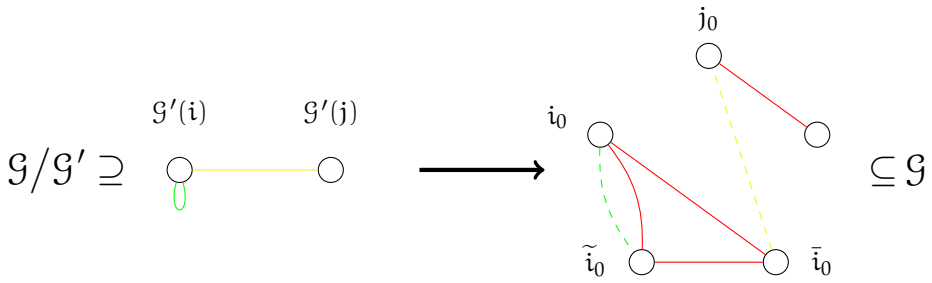

FIGURE 39. Example: final configuration for green loop edges in the quotient, first case (I).

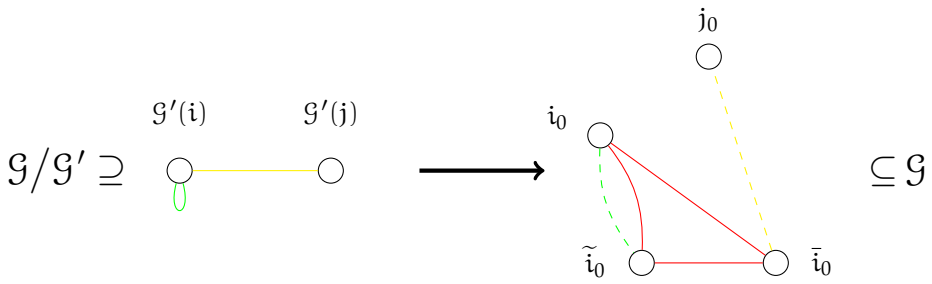

FIGURE 40. Example: final configuration for green loop edges in the quotient, second case (I).

In both cases, reasoning as in the proof of the second case of Lem. 6.1, the subgraphs $\mathcal{G}'(i), \mathcal{G}'(j) \subseteq \mathcal{G}'$ are then contained in a bichromatic component of $\mathcal{G}$. Hence the straight edge $\{ \mathcal{G}'(i), \mathcal{G}'(j) \}$ will double in the quotient, but if $\mathcal{G}'(j)$ is trivial the green loop edge $\{ \mathcal{G}'(j) \}$ need *not* arise in $\mathcal{G}/\mathcal{G}'$ (compare the following with Figg. 34 and 35):

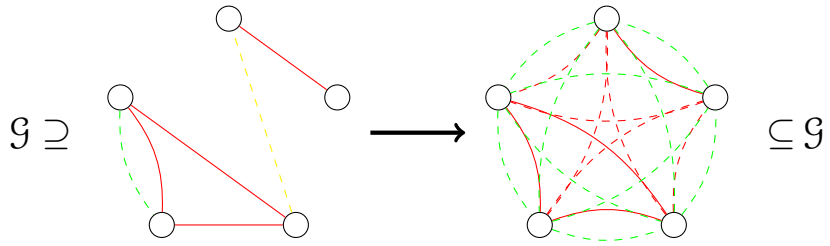

FIGURE 41. Example: final configuration for green loop edges in the quotient, first case (II).

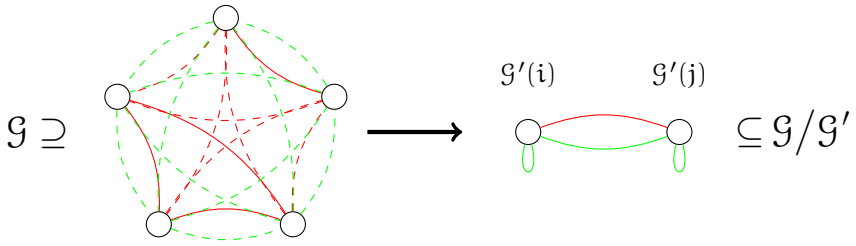

FIGURE 42. Example: final configuration for green loop edges in the quotient, first case (III).

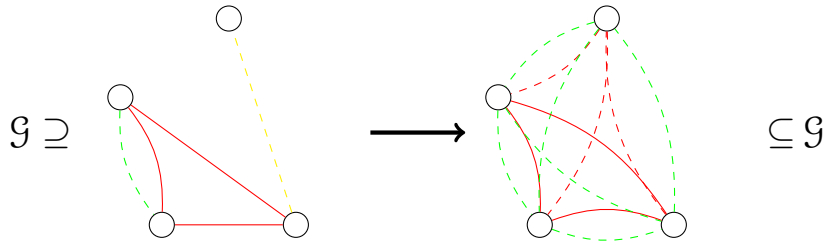

FIGURE 43. Example: final configuration for green loop edges in the quotient, second case (II).

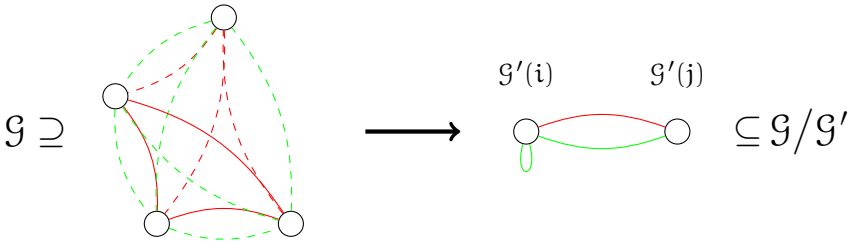

FIGURE 44. Example: final configuration for green loop edges in the quotient, second case (III).

This completes the proof of Thm. 6.2.

6.2. **Exotic components.** It follows that there are two new connected components of quasi-crystallographs: starting from a component of type B or D, we can glue green loop edges to any subset of nodes. For integers $r, s \geqslant 0$ we will say these are bichromatic graphs of type $B_{r+s}C_r$ and C_rD_{r+s}, respectively, where r is the number of nodes with green loop edges, and s the number of nodes without—so they have $n = r + s$ nodes, and we have the tautological identities $B_rC_r = BC_r$, $B_sC_0 = B_s$, $C_0D_s = D_s$ and $C_rD_r = C_r$.

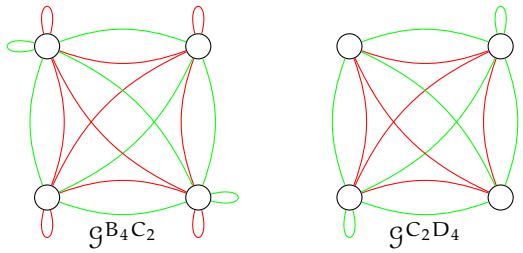

FIGURE 45. Examples of "exotic" quasi-crystallographs.

Remark 6.1. The hyperplane arrangement associated with the symmetric subset $\Phi^{B_{r+s}C_r} \subseteq BC_n$ is of type B_n/C_n, where $n = r + s$, so this is always crystallographic. The point is dilating any linear functional will not change the arrangement, so there is no difference in having one or two loop edges at a node.

On the contrary there *is* a difference between having zero or one loop edges, so $\Phi^{C_r D_{r+s}} \subseteq BC_n$ leads to an "exotic" hyperplane arrangement, which is not always crystallographic (as mentioned above). We say it is of type $(B_r/C_r)D_{r+s}$—slightly changing the notation of [16]. △

Putting all together we have proven the following classification of quasi-cristallographs, in view of Thm. 4.1.

Corollary 6.1. *All quasi-crystallographs are disjoint unions of bichromatic graphs of type* A_n, B_n, C_n, D_n, BC_n, $B_{r+s}C_r$ *or* C_rD_{r+s}, *for integers* $n, r, s \geqslant 0$.

Finally we can prove the converse of Thm. 6.2, so that in the end this is a classification of all possible restrictions (6) of root systems onto the kernels of their subsystems—which was one of the main goals.

Proposition 6.2. *All quasi-crystallographs are quotient graphs.*

Proof. By Cor. 6.1, it is enough to prove the statement for all components, since taking quotients and disjoint unions of crystallographs are commutative operations: if $\mathcal{G}' = \coprod_I \mathcal{G}'_i$ is a subgraph of $\mathcal{G} = \coprod_I \mathcal{G}_i$, so that $\mathcal{G}'_i \subseteq \mathcal{G}_i$ for $i \in I$, then by definition

$$\mathcal{G}/\mathcal{G}' = \coprod_I \mathcal{G}_i/\mathcal{G}'_i\,.$$

Moreover if $\mathcal{G}'$ is a totally disconnected graph on $n \geqslant 1$ nodes then $\mathcal{G}/\mathcal{G}' = \mathcal{G}$, so certainly all crystallographic components arise.

Finally consider the crystallograph $\mathcal{G}_{r,s}$ obtained as the disjoint union of $r \geqslant 0$ graphs of type A_1, and $s \geqslant 0$ graphs of type A_0:

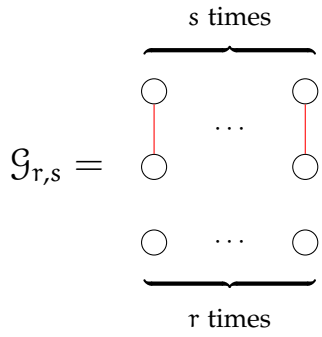

FIGURE 46. The graph $\mathcal{G}_{r,s}$.

This is naturally embedded as a subgraph of both B_{r+2s} and D_{r+2s}, and one readily verifies that

$$\mathcal{G}^{B_{r+2s}}/\mathcal{G}_{r,s} = \mathcal{G}^{B_{r+s}C_r}\,, \qquad \mathcal{G}^{D_{r+2s}}/\mathcal{G}_{r,s} = \mathcal{G}^{C_rD_{r+s}}\,.$$

Indeed in both cases the quotient has $r+s$ nodes and all possible straight edges, and in the former case it also has all red loop edges; finally there are s green loop edges at the nodes corresponding to the nontrivial red components of $\mathcal{G}_{r,s}$—and no other. □

Hence in conclusion all the information about restricted hyperplane arrangements is encoded in a quasi-crystallograph, but there is some clear redundancy that will be taken care of in the next section.

7. Hyperplane arrangements

Of course $\mathrm{Ker}(\Phi) \subseteq V$ only depends on $\Phi \subseteq V^\vee \setminus \{0\}$ up to dilation of each covector, i.e. on the subset $\mathbb{P}(\Phi) \coloneqq \pi(\Phi) \subseteq \mathbb{P}(V^\vee)$ of the projective dual space, using the canonical projection

$$\pi\colon V^\vee \setminus \{0\} \longrightarrow \mathbb{P}(V^\vee) =: (V^\vee \setminus \{0\})/\mathbb{C}^\times .$$

In particular in our situation we may restrict to positive systems $\Phi_+ \subseteq \Phi$ of roots, and further to reduced ones.

Now the bichromatic graph of a root system is already naturally associated with a choice of a positive system, since it has one (unoriented) edge for each opposite pair $\pm\alpha \in \Phi$; on the contrary we kept track of short/long roots for non-simply-laced types, by having loop edges of two different colours, which now ought to be fused into a single loop edge (of a different colour).

Introduce thus the extended set of (primary) colours $\{\mathsf{R}, \mathsf{G}, \mathsf{B}\}$, where now "blue" is allowed.

Definition 7.1. A *trichromatic* graph is a graph $\mathcal{G} = (\mathcal{G}_0, \mathcal{G}_1, \mathfrak{m})$ equipped with a colour function $c\colon \mathcal{G}_1 \to \{\mathsf{R}, \mathsf{G}, \mathsf{B}\}$, such that $c(e, \mathfrak{m}_e) \neq c(e', \mathfrak{m}_{e'})$ if $e = e' \subseteq \mathcal{G}_0$.

A trichromatic *subgraph* of $(\mathcal{G}, c)$ is a subgraph $\mathcal{G}' \subseteq \mathcal{G}$ equipped with the restricted colour function $c' = c\big|_{\mathcal{G}'_1}$.

By definition bichromatic graphs are (all the) trichromatic graphs $(\mathcal{G}, c)$ with $c(\mathcal{G}_1) \subseteq \{\mathsf{R}, \mathsf{G}\}$. This way the relevant terminology about bichromatic graphs can be naturally translated here—e.g. being simply-laced (= loopless), etc.

Now our viewpoint is that the adjacency of a trichromatic graph on $n \geqslant 1$ nodes can be used to encode certain hyperplane arrangements in $V = \mathbb{C}^n$, viz. certain lines in $V^\vee$, as follows. For $i \neq j \in \underline{n}$ denote

$$H_{ij}^{\pm} \coloneqq \mathrm{Ker}(\alpha_{ij}^{\pm}) = \left\{ \sum_k \alpha_k e_k \in V \;\middle|\; \alpha_i \pm \alpha_j = 0 \right\} \subseteq V ,$$

and

$$H_i \coloneqq \mathrm{Ker}(\alpha_i) = \left\{ \sum_k \alpha_k e_k \;\middle|\; \alpha_i = 0 \right\} \subseteq V ,$$

identifying the covectors $\alpha_i = e_i^\vee \in V^\vee$ with the linear coordinates $V \to \mathbb{C}$ in the basis $(e_1, \ldots, e_n)$. Then the root-hyperplane arrangements of the classical root systems are

$$\mathcal{H}^{\mathrm{A}_{n-1}} = \left\{ H_{ij}^- \;\middle|\; i \neq j \in \underline{n} \right\} , \quad \mathcal{H}^{\mathrm{D}_n} = \mathcal{H}^{\mathrm{A}_{n-1}} \cup \left\{ H_{ij}^+ \;\middle|\; i \neq j \in \underline{n} \right\} \subseteq \mathbb{P}(V^\vee) ,$$

and

$$\mathcal{H}^{\mathrm{B}_n} = \mathcal{H}^{\mathrm{C}_n} = \mathcal{H}^{\mathrm{BC}_n} = \mathcal{H}^{\mathrm{D}_n} \cup \{ H_i \mid i \in \underline{n} \} \subseteq \mathbb{P}(V^\vee) .$$

Now if $\mathcal{H} \subseteq \mathcal{H}^{\mathrm{BC}_n}$ we associate a trichromatic graph $\mathcal{G}^{\mathcal{H}}$ with it. It has nodes $\mathcal{G}_0^{\mathcal{H}} = \underline{n}$, and its adjacency/colouring are prescribed as follows:

(1) if $H_{ij}^- \in \mathcal{H}$, put a red straight edge $e = \{i, j\} \in \mathcal{G}_1^{\mathcal{H}}$;

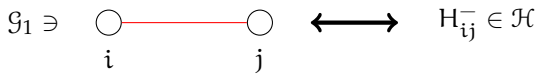

FIGURE 47. Projective correspondence, straight edges (I).

(2) if $H_{ij}^+ \in \mathcal{H}$, put a green straight edge $e = \{i, j\} \in \mathcal{G}_1^{\mathcal{H}}$;

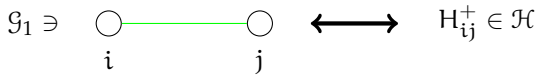

FIGURE 48. Projective correspondence, straight edges (II).

(3) if $H_k \in \mathcal{H}$, put a blue loop edge $l = \{k\} \in \mathcal{G}_1^{\mathcal{H}}$.

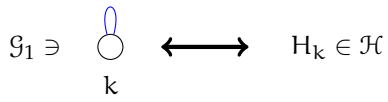

FIGURE 49. Projective correspondence, loop edges.

The conditions for the straight edges are completely analogous to the bichromatic case of § 2, while the case of loop edges should be compared with Figg. 4 and 5 (which are now "fused").

Remark 7.1. Just as in the case of root systems, a disjoint-union decomposition of $\mathcal{G}^{\mathcal{H}}$ corresponds to a direct sum decomposition of $\mathcal{H}$, and the number of hyperplanes is $|\mathcal{H}| = \left|\mathcal{G}_1^{\mathcal{H}}\right|$ (cf. Rk. 3.1). △

The above prescription singles out a special class of trichromatic graphs, which are in natural inclusion-preserving bijection with sub-arrangements of the root-hyperplane arrangement of type B/C: in particular $\overline{\mathcal{G}^{\mathcal{H}}} \subseteq \mathcal{G}^{\mathcal{H}}$ is a (simply-laced) bichromatic graph as above, and the full graph is obtained by glueing blue loop edges at some nodes.

Example 7.1. The classical root-hyperplane arrangements yields the following trichromatic graphs: the same bichromatic graphs as in Ex. 2.1 for the simply-laced cases, and a simply-laced complete bichromatic graph with blue loop edges glued at each node for types B/C/BC. Hence all non-simply-laced cases are "fused" into a single one; see below the case on $n = 4$ nodes:

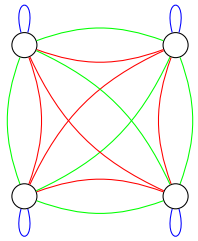

$$\mathcal{G}^{\mathcal{H}_{B_4}} = \mathcal{G}^{\mathcal{H}_{C_4}} = \mathcal{G}^{\mathcal{H}_{BC_4}}$$

FIGURE 50. Example: the rank-four non-simply-laced "classical" trichromatic graph.

△

Of course not all subsets $\mathcal{H} \subseteq \mathcal{H}^{BC_n}$ correspond to *root*-hyperplane arrangements, i.e. they are not the projectification of root subsystems $\Phi \subseteq BC_n$ (and so are *not* closed under mutual reflections): but those which do happen to be crystallographic are captured by a variation of the main definition.

Definition 7.2. A *projective* crystallograph is a trichromatic graph $(\mathcal{G}, c)$ such that $c(\overline{\mathcal{G}}) \subseteq \{R, G\}$ and $c(l) = B$ for all loop edges $l \in \mathcal{G}_1$, and satisfying the two conditions of Def. 3.1.

By definition the "simply-laced" condition yields the same local pictures as in the bichromatic case, viz. Figg. 8 9 and 10. The conditions involving loop edges instead become the following (compare with Figg. 11, 12, 13 and 14):

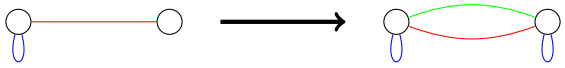

FIGURE 51. Loop edge closure condition for projective crystallographs (I).

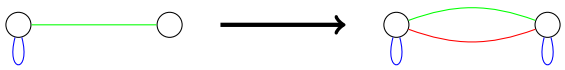

FIGURE 52. Loop edge closure condition for projective crystallographs (II).

Any such graph is associated with a root-hyperplane arrangement $\mathcal{H} = \mathcal{H}^{\mathcal{G},c}$, inverting the above prescription.

Then running the same argument in the proof of Thm. 4.1 yields the following classification.

Corollary 7.1. *Let $(\mathcal{G},c)$ be a projective crystallograph on $n \geqslant 1$ nodes. Then $\mathcal{G}$ is a disjoint union of the "classical" (projective crystallo)graphs $\mathcal{G}^{\mathcal{H}_{A_{m-1}}}$, $\mathcal{G}^{\mathcal{H}_{D_m}}$ and $\mathcal{G}^{\mathcal{H}_{B_m}} = \mathcal{G}^{\mathcal{H}_{C_m}} = \mathcal{G}^{\mathcal{H}_{BC_m}}$ $(m \leqslant n)$, and of the simply-laced bichromatic graphs $\mathcal{G}^{d_1,d_2}$ $(d_1+d_2 \leqslant n)$.*

Again up to acting via the Weyl group we can restrict to "classical" components only (cf. Lem. 4.1).

The last idea is that there is a natural operation on graphs which mimics taking the projection $\pi\colon V^\vee \setminus \{0\} \to \mathbb{P}(V^\vee)$. Namely, if $(\mathcal{G},c)$ is *bi*chromatic, we can associate to it a *tri*chromatic graph by replacing all red/green loop edges by a (single) blue loop edge. The resulting trichromatic graph is denoted $\mathbb{P}(\mathcal{G},c)$, and called its *projectivisation*; see an example below:

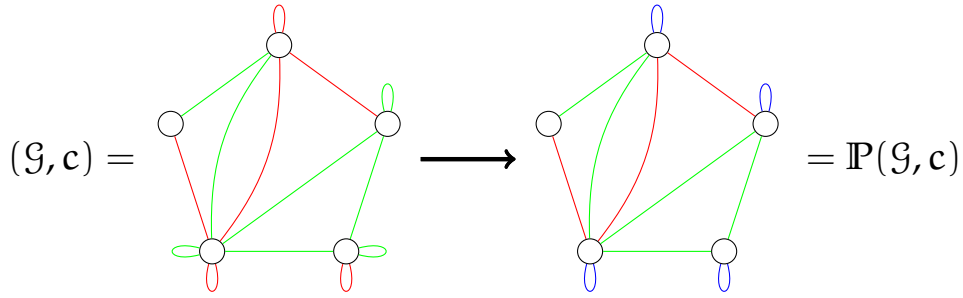

FIGURE 53. Example: projectivisation of a bichromatic graph.

Now if $\mathcal{G} = \mathcal{G}^\Phi$ for some symmetric subset $\Phi \subseteq V^\vee$ (in the dual reading), then $\mathbb{P}(\mathcal{G})$ encodes the projectivisation $\mathbb{P}(\Phi) \subseteq \mathbb{P}(V^\vee)$: indeed this latter is obtained by replacing each pair $\pm\alpha \in \Phi$ of opposite roots with the line it generates, i.e. with the hyperplane $\mathrm{Ker}(\pm\alpha) \subseteq V$, so in particular the overall operation "fuses" the short/long roots $\alpha_i, 2\alpha_i \in V^\vee$ into a single element—the new blue loop edge.

Theorem 7.1. *A sub-arrangement $\mathcal{H} \subseteq BC_n$ is crystallographic if and only if $\mathcal{G}^{\mathcal{H}}$ is a projective crystallograph, or equivalently if and only if it is the projectification of a crystallograph.*

Proof. The first statement is a corollary of Thm. 3.1, since the Weyl element associated to α_i and $2\alpha_i$ are the same for $i \in \underline{n}$.

The second statement follows from the classifications of Thm. 4.1 and Cor. 7.1. For the less trivial implication suppose $(\mathcal{G},c)$ is a projective crystallograph: then repainting its (blue) loop edges—if any—in red provides a "lifted" bichromatic graph $(\widetilde{\mathcal{G}},\widetilde{c})$ such that $\mathbb{P}(\widetilde{\mathcal{G}},\widetilde{c}) = (\mathcal{G},c)$, and this latter is a crystallograph. [8] □

Hence up to isomorphism we obtain a classification of the hyperplane arrangements of root subsystems of all classical root systems, reading from Cor. 4.1: in particular they are direct sums of classical root-hyperplane arrangements.

[8] Of course other lifts are possible, e.g. putting green loop edges, which corresponds to the fact that the (dual) root systems of type B and C have the same root-hyperplane arrangement.

7.1. **About quotients.** Finally an analogous variation of the main definition can be given for quasi-crystallographs, with a view towards encoding the hyperplane arrangements of quotients of root systems.

Namely we can define the quotient of two nested projective crystallographs using the same algorithm of Def. 6.1, but replacing red/green loop edges with blue loop edges throughout.

Example 7.2 (Adjacency of a quotient of projective crystallographs). Compare the following pictures with those of Ex. 6.1.

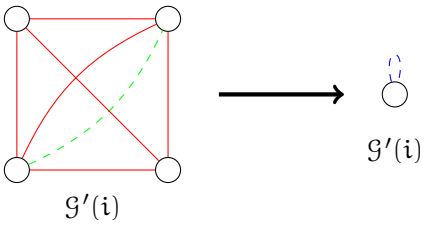

FIGURE 54. Example: loop edge in $\mathcal{G}/\mathcal{G}'$, arising from a green straight edge within a red component of $\mathcal{G}'$.

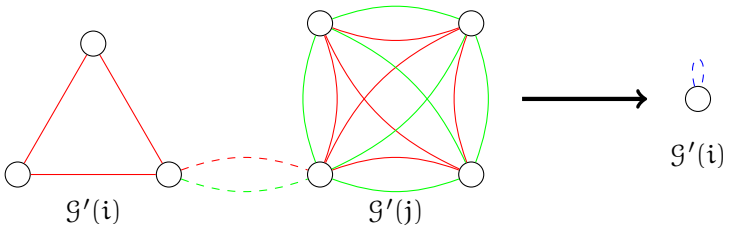

FIGURE 55. Example: loop edge in $\mathcal{G}/\mathcal{G}'$, arising from a straight edge from a red component to a bichromatic component of $\mathcal{G}'$.

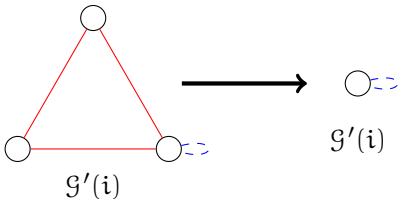

FIGURE 56. Loop edge in $\mathcal{G}/\mathcal{G}'$, arising from a loop edge within a red component of $\mathcal{G}'$.

△

By construction the resulting graph has no blue straight edges, and no red/green loop edges, but it need not be a projective crystallograph. Nonetheless this definition leads to the following compatibility.

Lemma 7.1. *Projectifications and quotients of crystallographs are commutative operations: if $\mathcal{G}' \subseteq \mathcal{G}$ are nested crystallographs then there is an equality*

$$\mathbb{P}(\mathcal{G})/\mathbb{P}(\mathcal{G}') = \mathbb{P}\big(\mathcal{G}/\mathcal{G}'\big)\,, \tag{14}$$

of trichromatic graphs.

Proof. The set of nodes are the same, since (simply-laced) red components of $\mathcal{G}'$ are unaffected by operation $\mathcal{G} \mapsto \mathbb{P}(\mathcal{G})$. As for the adjacency/colouring, by the same token the simply-laced parts of both sides of (14) coincide, so we need only show that the subsets of nodes with blue loop edges are the same.

Now let $\mathcal{G}'(i) \subseteq \mathcal{G}'$ be a red component. By definition the left-hand side of (14) has a blue loop edge $l = \{\, \mathcal{G}'(i) \,\}$ if and only if:

- there is a straight green edge $e \in \mathcal{G}_1$ within $\mathcal{G}'(i)$;
- there is a straight edge $e \in \mathcal{G}_1$ from $\mathcal{G}'(i)$ to a bichromatic component of $\mathcal{G}'$;
- there is a loop at a node of $\mathcal{G}'(i)$.

In all these cases there will be a loop $l = \{\, \mathcal{G}'(i) \,\}$ (of the same colour) in the quotient $\mathcal{G}/\mathcal{G}'$, reasoning as in the proofs of the lemmata in § 6: this becomes blue after projectification—i.e. on the right-hand side of (14). □

Hence the quotients of projective crystallographs are exactly the projectifications of quasi-crystallographs, in view of Thm. 6.2 and Prop. 6.2. In turn the two "exotic" components of Cor. 6.1 only yield one "exotic" hyperplane arrangement, corresponding to a simply-laced complete bichromatic graph with blue loop edges glued at any *proper* subset of nodes (cf. Rk. 6.1).

This leads to the final statement, classifying *all* restricted root-hyperplane arrangements.

Theorem 7.2. *Let $\Phi' \subseteq \Phi \subseteq BC_n$ be nested root systems. Then the hyperplane arrangement of the restricted system (6) is isomorphic to a direct sum of hyperplane arrangements of classical type, or of (unique) "exotic" type $(B_r/C_r)D_{r+s}$, for integers $r, s \geqslant 0$—with $r + s \leqslant n$.*

Outlook

The Borel–de Siebenthal theory [10] classifies connected closed subgroups of maximal rank, inside connected compact Lie groups G—with a given maximal torus $T \subseteq G$. This can be expressed in terms of certain operations on the extended Dyinkin diagram of $\mathfrak{g} = \mathrm{Lie}(G)$, and leads in particular to a classification of maximal closed subsystems of $\Phi_{\mathfrak{g}}$, cf. [19].

The present graph-theoretic construction instead does *not* rely on (extended) Dynkin diagrams, but rather replaces them with new combinatoric objects that retain more information. In particular we thus classify root subsystems of *any* rank, not just maximal ones (cf. [24]); in principle a Lie-group theoretic analogue should exist. Moreover in our viewpoint maximal root subsystems simply

correspond to maximal sub-crystallographs, so can still be characterised in combinatoric fashion, encompassing e.g. maximal simply-laced complete subgraphs in type A.

Data availability

Data sharing not applicable to this article as no datasets were generated or analysed during the current study.

Appendix A. Notations/conventions

Graphs. A *multiset* is a set S with a multiplicity function $m\colon S \to \mathbb{Z}_{\geqslant 1}$. If the underlying set S is finite then $|m| = \sum_{i\in S} m(i) \in \mathbb{Z}_{\geqslant 1}$ is the *cardinality* of (S, m).

A *graph* is a triple $\mathcal{G} = (\mathcal{G}_0, \mathcal{G}_1, m)$ consisting of a set of *nodes* $\mathcal{G}_0$ and a multiset $(\mathcal{G}_1, m)$ of (unoriented) *edges*. In turn an edge is a multiset (e, m_e) with $|m_e| = 2$, and such that its underlying set lies in $\mathcal{G}_0$: it is a *loop edge* if e is a singleton, else it is a *straight edge*. The forgetful function $\mathcal{G}_1 \to \mathcal{P}(\mathcal{G}_0)$ defined by $(e, m_e) \mapsto e$ is the *incidence* of the graph: the edge (e, e_m) is incident at the node(s) of $e \subseteq \mathcal{G}_0$, and conversely.

A straight edge incident at the nodes $i \neq j \in \mathcal{G}_0$ is written $e = \{i, j\} \in \mathcal{G}_1$—with $m(i) = m(j) = 1$—, while a loop edge incident at $k \in \mathcal{G}_0$ is $l = \{k\}$—with $m(k) = 2$. These are depicted as customary:

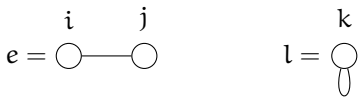

Figure 57. Straight and loop edges

A *subgraph* $\mathcal{G}'$ of $\mathcal{G}$ is obtained by removing some node or edge: if a node is removed all its adjacent edges are also dropped, and the resulting partial order is denoted $\mathcal{G}' \subseteq \mathcal{G}$.

The disconnected/disjoint union of two graphs $\mathcal{G}$ and $\mathcal{G}'$ is denoted $\mathcal{G} \amalg \mathcal{G}'$, and underlies the disjoint union $\mathcal{G}_0 \amalg \mathcal{G}'_0$ of the sets of nodes.

Root systems and Weyl groups. For an integer $n \geqslant 1$ let $V = \mathbb{C}^n$ with canonical basis $(e_1, \dots, e_n)$—and scalar product $(e_i \mid e_j) = \delta_{ij}$, whenever helpful. There are finite subsets

$$A_{n-1} \subseteq D_n \subseteq B_n, C_n \subseteq BC_n \subseteq V \setminus \{0\}\,,$$

of nested (crystallographic, irreducible) root systems, defined as follows. If $e^{\pm}_{ij} \coloneqq e_i \pm e_j \in V$ for $i, j \in \underline{n} = \{1, \dots, n\}$, then

$$A_{n-1} = \left\{ e^-_{ij} \;\middle|\; i \neq j \in \underline{n} \right\}, \qquad D_n = A_{n-1} \cup \left\{ \pm e^+_{ij} \;\middle|\; i \neq j \in \underline{n} \right\},$$

and

$$B_n = D_n \cup \{ e_i \mid i \in \underline{n} \}, \qquad C_n = D_n \cup \{ 2e_i \mid i \in \underline{n} \},$$

and finally $BC_n = B_n \cup C_n$.

The single-letter families are the classical *reduced* root systems, while BC_n is a *nonreduced* irreducible root system—the unique one of rank n, up to isomorphism, cf. [11, Ch. VI] and [18].

There is a dual viewpoint where $BC_n \subseteq V^\vee$, consisting of covectors naturally associated with the dual basis $\alpha_i = e_i^\vee \in V^\vee$—i.e. taking dual/inverse root systems. Whenever helpful we equip $V^\vee$ with the push-forward scalar product along the vector space isomorphism $(\cdot \mid \cdot)^\flat \colon V \to V^\vee$, and we identify (canonically) the Weyl groups $W(\Phi) \subseteq \mathrm{GL}(V)$ and $W(\Phi^\vee) \subseteq \mathrm{GL}(V^\vee)$ by $w \mapsto {}^t w^{-1}$.

The association of Weyl reflections to roots is denoted $\alpha \mapsto \sigma_\alpha$.

A root *subsystem* of a root system $\Phi \subseteq V$ is a subset $\Phi' \subseteq \Phi$ such that $\sigma_\alpha(\Phi') \subseteq \Phi'$ for $\alpha \in \Phi'$. The Weyl group permutes root subsystems: two such are *equivalent* if they lie in the same Weyl-group orbit. This is a stricter relation than that of isomorphism, since there are in general "outer" automorphisms of Φ—the isomorphisms of the Dynkin diagram—which also preserve root subsystems.

Hyperplane arrangements. A (linear) *hyperplane arrangement* $\mathcal{H}$ in a finite-dimensional complex vector space V is a set of linear hyperplanes $H \subseteq V$: in this paper we only consider finite such arrangements, and we identify hyperplanes in V with lines in the dual space via $\lambda \mapsto \mathrm{Ker}(\lambda) \subseteq V$, for $\lambda \in V^\vee \setminus \{0\}$.

An isomorphism of two hyperplane arrangements $\mathcal{H}, \mathcal{H}'$ in V is a linear automorphism $w \in \mathrm{GL}(V)$ such that $\left\{ w(H) \;\middle|\; H \in \mathcal{H} \right\} = \mathcal{H}'$.

A *sub-arrangement* of $\mathcal{H} \subseteq \mathbb{P}(V^\vee)$ is a subset $\mathcal{H}' \subseteq \mathcal{H}$ of hyperplanes of $\mathcal{H}$.

The *direct sum* of hyperplane arrangements $\mathcal{H}_i \subseteq \mathbb{P}(V_i^\vee)$, $i = 1, 2$, is the set of hyperplanes

$$H_1 \oplus V_2,\ V_1 \oplus H_2 \subseteq V_1 \oplus V_2\,, \qquad H_i \in \mathcal{H}_i\,.$$

The hyperplane arrangement of a root-system $\Phi \subseteq V^\vee$—viz. a "root-hyperplane arrangement", for short—is the set

$$\mathcal{H}^\Phi \coloneqq \left\{ \mathrm{Ker}(\alpha) \;\middle|\; \alpha \in \Phi \right\} \simeq \Phi / \mathbb{C}^\times \subseteq \mathbb{P}(V^\vee)\,.$$

Such hyperplane arrangements are said to be *crystallographic*.

References

1. J. E. Andersen, A. Malusà, and G. Rembado, *Genus-one complex quantum Chern–Simons theory*, 2020, arXiv:2012.15630; submitted.
2. ———, *Sp(1)-symmetric hyperkähler quantisation*, 2021, arxiv:2111.03584; submitted.
3. O. Biquard and P. P. Boalch, *Wild nonabelian Hodge theory on curves*, Compos. Math. **140** (2004), no. 1, 179–204.
4. P. P. Boalch, *G-bundles, isomonodromy, and quantum Weyl groups*, Int. Math. Res. Not. (2002), no. 22, 1129–1166.
5. ———, *Quasi-Hamiltonian geometry of meromorphic connections*, Duke Math. J. **139** (2007), no. 2, 369–405.
6. ———, *Through the analytic Halo: fission via irregular singularities*, Ann. Inst. Fourier (Grenoble) **59** (2009), no. 7, 2669–2684.
7. ———, *Hyperkähler manifolds and nonabelian Hodge theory of (irregular) curves*, 2012, arXiv:1203.6607.
8. ———, *Geometry and braiding of Stokes data; fission and wild character varieties*, Ann. of Math. (2) **179** (2014), no. 1, 301–365.
9. ———, *Wild character varieties, meromorphic Hitchin systems and Dynkin diagrams*, Proceedings, Nigel Hitchin's 70th Birthday Conference, Oxford University Press, 2017.
10. A. Borel and J. de Siebenthal, *Les sous-groupes fermés de rang maximum des groupes de Lie clos*, Comment. Math. Helv. **23** (1949), 200–221.
11. N. Bourbaki, *Éléments de mathématique. Fasc. XXXVII. Groupes et algèbres de Lie. Chapitres IV–VI*, Hermann, Paris, 1968.
12. E. Brieskorn, *Die Fundamentalgruppe des Raumes der regulären Orbits einer endlichen komplexen Spiegelungsgruppe*, Invent. Math. **12** (1971), 57–61.
13. E. Brieskorn and K. Saito, *Artin-Gruppen und Coxeter-Gruppen*, Invent. Math. **17** (1972), 245–271.

14. P. Deligne, *Les immeubles des groupes de tresses généralisés*, Invent. Math. **17** (1972), 273–302.
15. S. Dijols, *Projection of root systems*, 2019, arXiv:1904.01884.
16. J. Douçot, G. Rembado, and M. Tamiozzo, *Local wild mapping class groups and cabled braids*, 2022, arXiv:2204.08188; submitted.
17. G. Felder and G. Rembado, *Singular modules for affine Lie algebras, and applications to irregular WZNW conformal blocks*, 2020, arXiv:201214793; to appear in *Selecta Mathematica*.
18. J. E. Humphreys, *Introduction to Lie algebras and representation theory*, Springer-Verlag, New York-Berlin, 1972, Graduate Texts in Mathematics, Vol. 9.
19. R. Kane, *Reflection groups and invariant theory*, CMS Books in Mathematics/Ouvrages de Mathématiques de la SMC, vol. 5, Springer-Verlag, New York, 2001.
20. T. Oshima, *A classification of subsystems of a root system*, 2006, arXiv:math/0611904.
21. G. Rembado, *Quantisation of moduli spaces and connections*, Ph.D. thesis, Université de Paris-Sud, 2018, available at tel-02004685.
22. ———, *Simply-laced quantum connections generalising KZ*, Comm. Math. Phys. **368** (2019), no. 1, 1–54.
23. ———, *Symmetries of the simply-laced quantum connections and quantisation of quiver varieties*, SIGMA Symmetry Integrability Geom. Methods Appl. **16** (2020), Paper No. 103, 44.
24. N. R. Wallach, *On maximal subsystems of root systems*, Canadian J. Math. **20** (1968), 555–574.

(G. Rembado) Hausdorff Centre for Mathematics, University of Bonn, 60 Endenicher Allee, D-53115 Bonn (Germany)

Email address: gabriele.rembado@hcm.uni-bonn.de